UNIVERSITY OF CALIFORNIA

Santa Barbara

Synthesis and Characterization of Metal-Oxo Phthalocyanine Complexes

A Thesis submitted in partial satisfaction of

the requirements for the degree Master of Science

in Chemistry

by

Christopher Joseph Kirby Jr.

Committee in Charge:

Professor Gabriel Ménard, Chair

Professor Trevor W. Hayton

Professor Alison Butler

June 2018

The thesis of Christopher Joseph Kirby Jr. is Approved.

Professor Trevor W. Hayton

Professor Alison Butler

Professor Gabriel Ménard, Committee Chair

June 2018

Synthesis and Characterization of Metal-Oxo Phthalocyanine Complexes

Dedications/Acknowledgements:

I would like to take this opportunity to first thank Dr. Gab Menard, for his guidance, mentorship and patience over the last three years. I wouldn't be here without him and his aid.

A thank you to the Gab Lab group members who have always been an invaluable resource of wealth and knowledge. A special thanks to the first members: Camden Hunt, Megan Keener, and Tim Carroll, who have all been supportive throughout this process. A thanks to Camden Hunt, Maddy Peterson, and Zongheng Wang, for help with starting materials and other things as we all worked on phthalocyanine species.

Thanks to all the other chem faculty and staff. A thanks to the guys down in the machine shop and in the stockroom who were always very helpful and friendly when it came to getting glassware, deliveries, and other appliances/tools. In the trailers, a special thanks to India Madden for all her help with all paperwork and guidance throughout this process. A thanks to Adrian who was always a close friend that was nice to chat with on a rough day. Lastly, a thanks to Dmitri, who I wish was around a lot longer than he was, as his help with Mass Spectrometry was invaluable.

A thanks to my other friends in the Chemistry department, Kyle, Jamie, Meghan, Greg, Sierra, Jacob, Austin, Andrew, Andre, Alex, Aneta, Manny, and many others. I will miss playing basketball with the Bucky Ballers, gossiping over some barbeque, and countless stories told while we were TAing together.

A thanks to my friends and mentors from TCNJ, especially: Dr. Hunt, Dr. Bradley, Dr. O'Connor, Craig, Otto, Jimmy Liam, Danny, Lea, and Danielle. Thank you

for the encouragement to come out to California and pursue an advanced degree. Thanks for helping me clear my mind by talking sports, life, and giving me advice along the way.

A special thanks to my family: my mom, my dad, Jenna, Cailey, Jackie and my Aunt Mary. Thanks for putting up with my long phone calls and the love and support that I needed to get to this point.

A thanks to my special friend Sabrina Solley who has helped me a lot throughout this long process. Thanks for bringing me food during those late nights in lab, when I didn't think I was going to make it home until really late and thank you for your love and support throughout this.

Lastly, I want to dedicate this work to my grandparents Baldy, Nanny, and Poppy. None of you got to see the end result, but your support over the years has been a godsend and I hope that you are watching me and smiling now.

ABSTRACT

Synthesis and Characterization of Metal-Oxo Phthalocyanine Complexes

by

Christopher Joseph Kirby Jr.

The synthesis of two substituted phthalocyanine ligands for synthesis of metal phthalocyanine complexes is reported. Both phthalocyanine ligands contain ethereal substitutions of differing size. One substitution is an ethoxy phthalocyanine species and the other is an isopropoxy phthalocyanine.

The synthesis and characterization of two vanadyl (IV) phthalocyanine species is reported. EPR data, mass spectrometry data and x-ray diffraction are included to characterize the vanadyl ethoxyphthalocyanine. The vanadyl isopropoxyphthalocyanine is characterized by mass spectrometry.

The synthesis and characterization of a chromium (II) phthalocyanine is reported. The species is characterized by NMR, mass spectrometry and x-ray diffraction. This species and its reactions with O atom donors are reported and the results are examined.

The synthesis and characterization of a manganese (III) chloride and a “naked” manganese (III) ethoxyphthalocyanine are reported. Mass spectrometry and NMR are used to characterize these two species. The reactions of these species with O atom donors

are reported and some preliminary data is examined to explore the potential formation of a manganese oxo phthalocyanine species.

TABLE OF CONTENTS

LIST OF FIGURES

Chapter 1 Phthalocyanines

1.1 Introduction

A heme is defined as an iron containing porphyrin that forms the non-protein portion of some biological molecules. Hemes are present in a multitude of proteins in nature, and within each of these proteins they perform a variety of different functions. For example, myoglobin and hemoglobin are proteins capable of binding oxygen reversibly. Myoglobin functions to store oxygen for use in muscle tissue, while hemoglobin works to transport it throughout the body in the bloodstream.[1]

There also exists an important class of heme metalloproteins, referred to as cytochrome P450 enzymes (**Figure 1.1**). These enzymes are used to catalyze a range of oxidative reactions *in vivo*, including: substrate hydroxylations, nitrogen atom transfer and olefin epoxidations.[2-3] Unlike myoglobin and hemoglobin, which are used to capture and transport oxygen throughout the body, these proteins are capable of binding oxygen and cleaving the O=O bond, thereby generating high-valent metal species capable of activating strong C–H bonds.[4] The high-valent species eluded scientists for years, and it was not until 2010 that the high-valent iron-oxo species was isolated and characterized.[5-6]

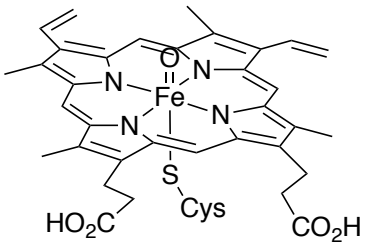

Figure 1.1. A heme protein in cytochrome P450. Iron holds a +4 charge in this species and a cysteine residue helps to balance out the charge on the iron-oxo.

1.2 Synthetic Molecular Mimics of Terminal Metal-Oxo Species

Many different ligands have been synthesized in order to generate a synthetic model of the natural species. Among these are porphyrins, which are identical to the

biological framework of the ligand seen in hemes. Corroles and phthalocyanines mimic porphyrins in that they contain the same square-planar motif of heme around the metal and would give a square-pyramidal structure on the addition of an oxo.

1.2.1 Porphyrin / Porphyrazines

Porphyrin rings are the name given to the ligand of heme proteins (**Figure 1.2a**). Porphyrins have been synthesized to be the most similar model complex for the various hemoproteins. Porphyrins and their analogs, such as porphyrazines (**Figure 1.2b**), consist of four pyrrole subunits connected in a cyclic form at their α-carbons by methine or nitrogen atom bridges, respectively.

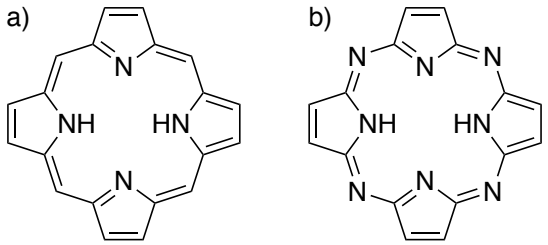

Figure 1.2. The structure of a (a) porphyrin and (b) porphyrazine ligand

The synthesis of porphyrin metal complexes capable of binding molecular oxygen have been known and cited in literature for decades.[7-14] Perhaps one of the more famous models of forming an iron dioxygen species, much like that of hemoproteins, is the "picket fence" porphyrin.[8-9, 15-20] The "picket fence" porphyrin (**Figure 1.3**) modelled the reversible oxygen binding seen in heme proteins such as oxymyoglobin and oxyhemoglobin. The porphyrin in this system forms its "picket fence" by substitution of ortho-pivalamidophenyl groups on the methine bridge in place of protons.[8] In the synthesis of this ligand, it is very important that the proper atropisomer is isolated. Atropisomerization is a form of stereoisomerization where free rotation around a single bond is obstructed due to steric strain. In the "picket fence" porphyrin, the bulk of the

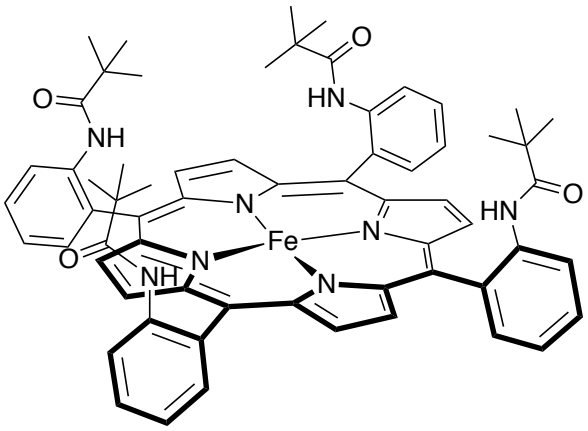

Figure 1.3. Molecular structure of the "picket fence" porphyrin. Note the ortho-pivalamidophenyl substituents, these serve to trap oxygen helping to bind O_2.

ortho-pivalamidophenyl group prevents its rotation around the bond of the phenyl to the bridging carbon. These groups serve to leave one axial site on the iron center completely open to binding of an axial base (similar to the histidine subunits in hemeproteins) while leaving a pocket on the opposite axial site to allow binding of dioxygen. This in turn prevents the reaction of two porphyrins with molecular oxygen.[8] This system serves as a suitable model for heme proteins such as myoglobin and hemoglobin as it shows the ability to bind and isolate a species with molecular oxygen.

Other models mimic different biological systems such as the manganese-oxo present in photosystem II in plants. The manganese oxo bond has been synthesized using porphyrins despite the differences in structure, as photosystem II is not a system containing a porphyrin. Specifically, the oxygen evolving complex within photosystem II has multiple manganese-oxo bonds including both terminal and bridging oxos. During photosynthesis this structure is responsible for the splitting of water to form dioxygen.[21-23] There have been multiple attempts to make similar systems and study the reactivity of manganese-oxo species using a porphyrin ligand framework.[24-30] One such manganese terminal oxo was seen to be a reactive oxidant (**Figure 1.4**).

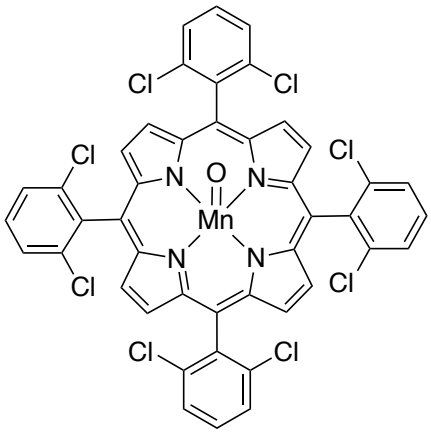

Figure: 1.4. Manganese(V) oxo porphyrin complex synthesized as an oxidation catalyst using m-CPBA.

The species was capable of forming phosphorus(V) oxides from phosphorus(III) species (**Scheme 1.1**).[27]

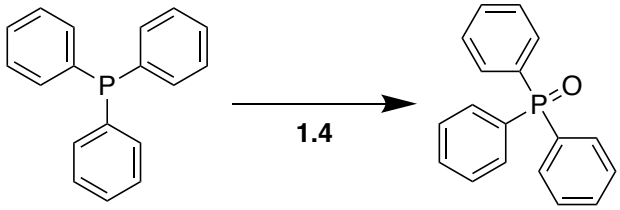

Scheme 1.1. Oxidation of triphenyl phosphine to triphenylphosphine oxide by **1.4**. Reaction takes place at room temperature.

Porphyrins have been a very useful ligand platform to mimic reactions that occur *in vivo*. In particular, the picket fence porphyrin is a very good mimic showing the ability of iron to bind dioxygen, much like myoglobin and hemoglobin. Other porphyrin systems that have been synthesized have shown the ability of metal oxo species to do oxidative chemistry.

1.2.2 Corroles / Corrolazines

Corroles and corrolazines (**Figure 1.5a** and **Figure 1.5b**) are a relatively new framework with many similarities to both phthalocyanines (*vide infra*) and porphyrins;

however, they differ in a few specific ways. These systems are related to the corrin ligand that is found in vitamin B12.[31-36] They contain four pyrrole rings, which are composed of three single atom linkages to each other on either α-carbon, and one direct linkage from α-carbon to α-carbon. In addition, these species act as LX_3-type ligand donors with an overall -3 charge compared with the typical L_2X_2-type donation (-2 charge) that general phthalocyanines and porphyrins contain. The differences between corrin-based ligands and porphyrins are helpful for modelling the proposed intermediates and transition states of hemes and other biological systems. This is due to the ligand's charge, as it enables the metals to achieve higher oxidations states.

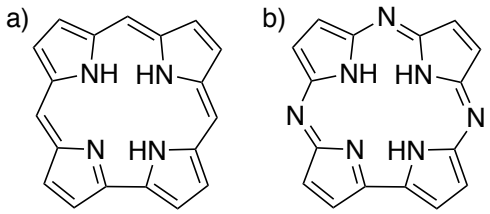

Figure 1.5. The structure of (a) corrole and (b) corrolazine

The corrolazine ligand (**Figure 1.5b**) was introduced by the Goldberg group at Johns Hopkins University as a means of simplifying the complex synthesis of corroles. The synthetic method of making this ligand is less involved, as it can be synthesized rather easily from a porphyrazine.[37] Corrolazines differ from corroles as they contain nitrogen atoms as the linker between pyrrole rings.

Using these frameworks, metalation of corroles and their derivative species is rather simple and has been accomplished using several first row metals, including: cobalt, copper, and vanadium.[38-40] Most relevant to this thesis are those of iron and manganese.[41-44] Iron or manganese corroles or corrolazines have been used to synthesize high-valent metal-oxo and amido species. These have been used for further chemical transformations

similar to that of the biological species that they mimic. For example, a manganese oxo species generated by the Goldberg group was first isolated on treatment of a manganese (III) corrolazine with *meta*-chloroperbenzoic acid (*m*-CPBA) (**Scheme 1.2**).[45]

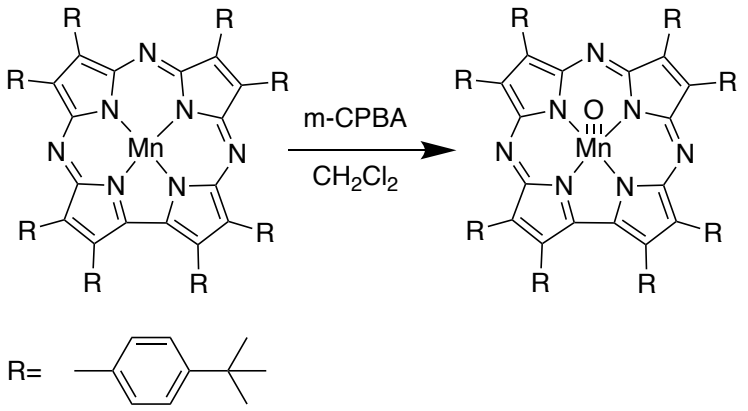

Scheme 1.2. Reaction of the manganese(III) corrolazine with an O-atom donor affords a manganese(V) oxo species. Alternatively use of dioxygen with UV light creates the same product. 1equivalent of m-CPBA, DCM, 25^{o}C, 1min.

Alternatively it was noted that this species can be generated under aerial oxidation with visible light.[46] A similar manganese-oxo corrole was synthesized and used to study C–H activation. The manganese-oxo corrole is capable of hydrogen atom transfer (HAT) as it extracts a single hydrogen to make the hydroxo (**Scheme 1.3a**), and then the hydroxo is able to extract a second hydrogen atom to form the aqua species (**Scheme 1.3b**). These manganese species are capable of oxidizing the substrate (in this case a series of phenol substrates) using both the oxo and hydroxo species.[47] In addition to these oxo species, an iron imido corrolazine similar to that of certain cytochrome enzymes was synthesized for use in the transfer of substituted amines. The iron imido is capable of transferring an NR group to various phosphine substrates affording the phospharane product.[44]

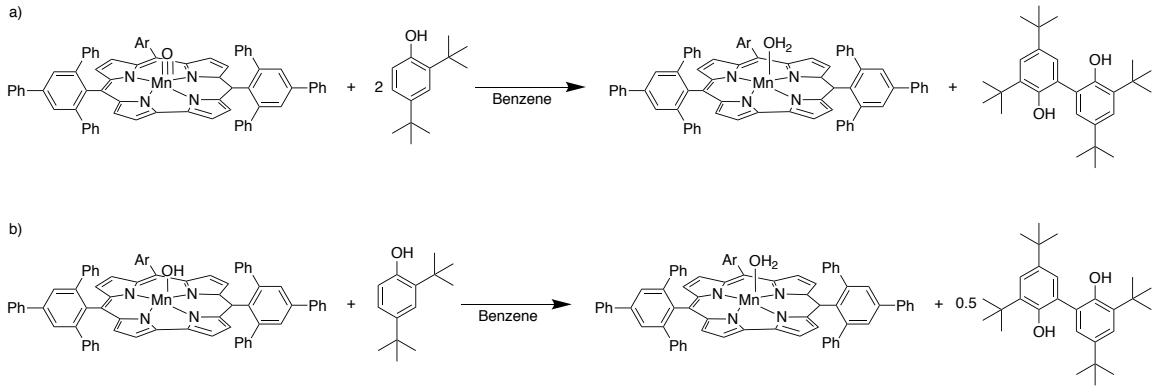

Scheme 1.3. C-H activation by (a) a manganese oxo (23°C) (b) a manganese hydroxo corrole (23°C). Both species are reactive with phenol substrates activating sp^2 C-H bonds.

Further modification of the corrole ligand has led to the creation of the hangman corrole (**Figure 1.6**). The hangman corrole is a unique form of corrole that was developed by the Nocera group in order to study oxygen reactions with corrole species.[48-53] The corrole they developed contains a side chain from the central linker of the pyrrole rings with groups available to aid in the bonding of an oxygen atom to the central metal.[50-51] In the cobalt(III) hangman corrole there is reactivity at the cobalt to first coordinate water. This complex is further capable of oxidizing water to dioxygen electrocatalytically. The mechanism of this transformation remains ambiguous, although the ability of the hangman group is beneficial for this process as it aids in the O–O bond formation.[49] DFT studies of this complex show that a metal oxo, reacting with water stabilized by the hangman portion of the molecule, is likely responsible for the ability of this complex to stabilize water oxidation reactions.[52]

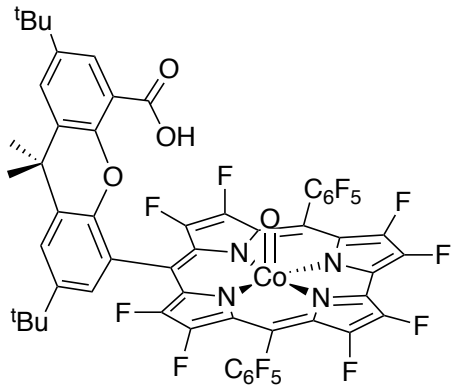

Figure 1.6. The structure of the cobalt hangman corrole, where a carboxylic acid helps in the binding of the water for oxidation, it also can help stabilize the oxo.

These two differing corrole derivatives are very unique, but show the ability of the metal to stabilize a metal oxo. The charge of the ligand aids in the ability of the metal to achieve higher oxidation states when compared with a porphyrin system. This is seen in the hangman case, where the ligand framework aids in the reactivity of the corrole because it is able to stabilize substrates for transformations with the complex.

1.2.3 Phthalocyanines

The phthalocyanine (Pc) is another synthetic derivative of heme proteins. They contain four benzo-fused pyrroles bound together by nitrogen linkers at the 1 and 4 positions of the pyrrole rings (**Figure 1.7**). The Pc ligand can exist in multiple oxidation states ranging from Pc(0) to Pc(-6), with the Pc(-2) oxidation state being most common, similar to porphyrins. These species are incredibly colorful and because of this have been often used as dyes and pigments.[54] The addition of benzene groups to the central porphyrazine core (**Figure 1.2b**) allows for facile incorporation of alkyl, aryl, halogen, and other functional groups to the periphery of the Pc ligand, allowing for precise control of steric and electronic parameters.[55] These substituents are also often very useful in solubilizing the poorly soluble bare Pc ligand.

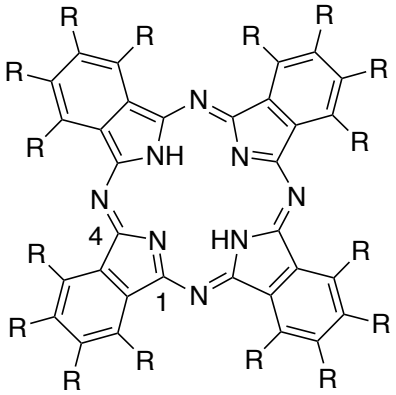

Figure 1.7. The structure of an unsubstituted and protonated form of the phthalocyanine.

Many transition metal Pc species (PcM) have been synthesized, and utilized to execute a diverse array of chemical transformations.[56] For example, PcM compounds have frequently been used in the electrochemical reduction of carbon dioxide.[57-61] Others have been used in oxidative processes such as methane oxidation and water oxidation.[62-65] The easily modified structure, as well as the extreme chemical stability of the ligand framework, makes PcM complexes suitable for numerous catalytic chemical processes.[56]

There are a very limited number of examples of PcM terminal-oxo species. The only two synthesized are vanadium oxo (vanadyl) and titanium oxo (titanyl).[66-69] The titanyl species has been studied as a possible water splitting agent. Titanyl phthalocyanines are capable of photooxidizing water to hydroxyl radicals upon excitation with UV light.[68] In terms of nitrides, there is only one known example of a terminal PcM nitride being synthesized.[70] This manganese nitride species is air stable and shows no signs of dimerization by formation of a bridged manganese nitride. Most oxo and nitride PcM complexes adopt bridging structures where an oxygen or nitrogen atom links two different phthalocyanines. One such example is the Cr–O–Cr phthalocyanine produced

by Leznoff (**Figure 1.8a**).[71] The chromium (II) species is oxidized to form a bridging oxygen on addition of an O-atom donor or alternatively in the presence of dioxygen.

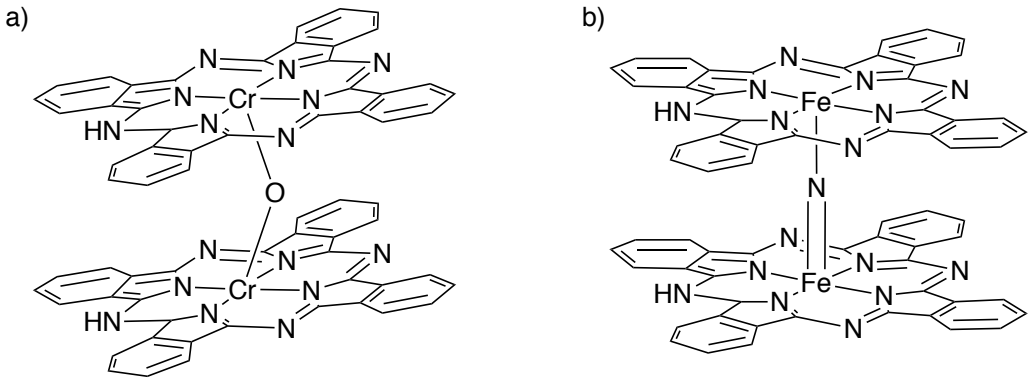

Figure 1.8. Examples of bridging species seen in phthalocyanines. (a) Leznoff's bridging chromium(III) phthalocyanine (coordinating THF excluded for clarity) (b) Sorokin's bridging iron nitride. The iron atoms both have a charge of 3.5+ due to delocalization across the Fe-N=Fe bonds.

In addition, Sorokin has done a lot of work with bridging nitride species (**Figure 1.8b**).[72-78] The bridging nitride species is capable of defluorination reactions and the oxidation of methane, among other transformations.[78] The catalyst is capable of activating C–F bonds as well as defluorinating aromatic species to a number of oxidized products in the presence of the catalyst and peroxide (**Scheme 1.4**).[76] Using peroxide to activate the phthalocyanine species allows the methane to be oxidized to methanol, formaldehyde, and formic acid. The primary product of this oxidation is methanol, though it can easily be converted under reaction conditions to formaldehyde and formic acid.[72] These species are likely to go through a terminal oxo intermediate, in which the bridging species helps to stabilize the terminal oxo in the octahedral intermediate.

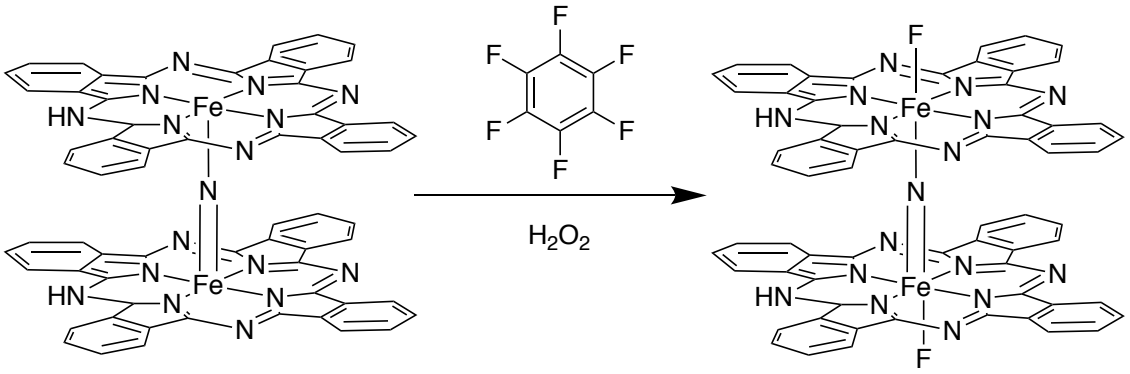

Scheme 1.4. Sorokin's iron nitride phthalocyanine is able to activate C-F bonds. Both Iron's become oxidized to Iron(IV) and one of the phthalocyanine rings becomes oxidized to $Pc^{+\bullet}$ while defluorinating the susbtrate.

1.3 Thesis Scope

Phthalocyanines have been understood to do a number of chemical transformations, as have their derivatives. The metal oxo bond that is often seen in other model complexes to cytochrome P450 seems to be the key in its reactivity. This thesis will outline our research to synthesize, isolate, and characterize a new class of metal-oxo species with potential to perform oxidative processes much like that of cytochrome P450. In Chapter 2, we describe the synthesis of metallated phthalocyanine species and also characterize them spectroscopically. In Chapter 3, we describe the synthesis of two vanadyl phthalocyanines, and discuss attempts at synthesizing a chromium and manganese oxo species. The work discussed in this thesis shows attempts towards synthesizing a metal oxo phthalocyanine species and the potential reactivity of such a species.

1.4 References

1. Marks, G. S., *Heme and Chlorophyll* D. Van Nostrand Company LTD: London, 1969.

2. Svastits, E. W.; Dawson, J. H.; Breslow, R.; Gellman, S. H., Functionalized Nitrogen Atom Transfer Catalyzed by Cytochrome-P-450. *J. Am. Chem. Soc.* **1985,** *107* (22), 6427-6428.

3. Meunier, B.; Bernadou, J., Metal-oxo species in P450 enzymes and biomimetic models. Oxo-hydroxo tautomerism with water-soluble metalloporphyrins. *Top. Catal.* **2002,** *21* (1-3), 47-54.

4. Cook, S. A.; Hill, E. A.; Borovik, A. S., Lessons from Nature: A Bio-Inspired Approach to Molecular Design. *Biochemistry* **2015,** *54* (27), 4167-4180.

5. Sligar, S. G., Glimpsing the Critical Intermediate in Cytochrome P450 Oxidations. *Science* **2010,** *330* (6006), 924-925.

6. Rittle, J.; Green, M. T., Cytochrome P450 Compound I: Capture, Characterization, and C-H Bond Activation Kinetics. *Science* **2010,** *330* (6006), 933-937.

7. Collman, J. P.; Gagne, R. R.; Kouba, J.; Ljusberg.H, Reversible Oxygen Adduct Formation in Cobalt(Ii) Picket-Fence-Porphyrins. *J. Am. Chem. Soc.* **1974,** *96* (21), 6800-6802.

8. Collman, J. P.; Gagne, R. R.; Reed, C. A.; Halbert, T. R.; Lang, G.; Robinson, W. T., Picket-Fence Porphyrins - Synthetic Models for Oxygen Binding Hemoproteins. *J. Am. Chem. Soc.* **1975,** *97* (6), 1427-1439.

9. Collman, J. P.; Brauman, J. I.; Doxsee, K. M.; Halbert, T. R.; Bunnenberg, E.; Linder, R. E.; Lamar, G. N.; Delgaudio, J.; Lang, G.; Spartalian, K., Synthesis and Characterization of Tailed Picket Fence Porphyrins. *J. Am. Chem. Soc.* **1980,** *102* (12), 4182-4192.

10. Odo, J.; Imai, H.; Kyuno, E.; Nakamoto, K., Resonance Raman-Spectra of Dioxygen Adducts of Cobalt Picket Fence Porphyrins. *J. Am. Chem. Soc.* **1988,** *110* (3), 742-748.

11. Wuenschell, G. E.; Tetreau, C.; Lavalette, D.; Reed, C. A., H-Bonded Oxyhemoglobin Models with Substituted Picket-Fence Porphyrins - the Model-Compound Equivalent of Site-Directed Mutagenesis. *J. Am. Chem. Soc.* **1992,** *114* (9), 3346-3355.

12. Lemaux, P.; Bahri, H.; Simonneaux, G., Preparation, Characterization and Reaction of the First Dioxoruthenium(Vi) Complexes of Chiral Picket-Fence Porphyrins. *J. Chem. Soc. Chem. Comm.* **1994,** (11), 1287-1288.

13. Smeets, S.; Asokan, C. V.; Motmans, F.; Dehaen, W., Synthesis and functionalization of double picket fence porphyrins starting from 4,6-disubstituted pyrimidine-5-carbaldehydes. *J. Org. Chem.* **2000,** *65* (18), 5882-5885.

14. Li, J. F.; Noll, B. C.; Oliver, A. G.; Schulz, C. E.; Scheidt, W. R., Correlated Ligand Dynamics in Oxyiron Picket Fence Porphyrins: Structural and Mossbauer Investigations. *J. Am. Chem. Soc.* **2013,** *135* (41), 15627-15641.

15. Collman, J. P.; Gagne, R. R.; Halbert, T. R.; Marchon, J. C.; Reed, C. A., Reversible Oxygen Adduct Formation in Ferrous Complexes Derived from a Picket Fence Porphyrin - Model for Oxymyoglobin. *J. Am. Chem. Soc.* **1973,** *95* (23), 7868-7870.

16. Collman, J. P.; Gagne, R. R.; Gray, H. B.; Hare, J. W., Low-Temperature Infrared Spectral Study of Iron(Ii) Dioxygen Complexes Derived from a Picket-Fence Porphyrin. *J. Am. Chem. Soc.* **1974,** *96* (20), 6522-6524.

17. Collman, J. P.; Gagne, R. R.; Reed, C. A., Paramagnetic Dioxygen Complex of Iron(Ii) Derived from a Picket Fence Porphyrin - Further Models for Hemoproteins. *J. Am. Chem. Soc.* **1974,** *96* (8), 2629-2631.

18. Jameson, G. B.; Robinson, W. T.; Collman, J. P.; Sorrell, T. N., Crystal and Molecular-Structure of a Novel, High-Spin, Iron(Ii) Picket Fence Porphyrin Derivative - Catena-(Mu-[Meso-Tetrakis(Alpha-Alpha-Alpha-Alpha-Ortho-Pivalamidophenyl)-Porphinato-N,N',N',N'-O]-Aquoiron(Ii)-Tetrahydrothiophene). *Inorg. Chem.* **1978,** *17* (4), 858-864.

19. Burke, J. M.; Kincaid, J. R.; Peters, S.; Gagne, R. R.; Collman, J. P.; Spiro, T. G., Structure-Sensitive Resonance Raman Bands of Tetraphenyl and Picket Fence Porphyrin-Iron Complexes, Including an Oxyhemoglobin Analog. *J. Am. Chem. Soc.* **1978,** *100* (19), 6083-6088.

20. Collman, J. P.; Brauman, J. I.; Iverson, B. L.; Sessler, J. L.; Morris, R. M.; Gibson, Q. H., O-2 and Co Binding to Iron(Ii) Porphyrins - a Comparison of the Picket Fence and Pocket Porphyrins. *J. Am. Chem. Soc.* **1983,** *105* (10), 3052-3064.

21. Baldwin, M. J.; Pecoraro, V. L., Energetics of proton-coupled electron transfer in high-valent Mn-2(mu-O)(2) systems: Models for water oxidation by the oxygen-evolving complex of photosystem II. *J. Am. Chem. Soc.* **1996,** *118* (45), 11325-11326.

22. Magnuson, A.; Frapart, Y.; Abrahamsson, M.; Horner, O.; Akermark, B.; Sun, L. C.; Girerd, J. J.; Hammarstrom, L.; Styring, S., A biomimetic model system for the water oxidizing triad in Photosystem II. *J. Am. Chem. Soc.* **1999,** *121* (1), 89-96.

23. Najafpour, M. M.; Heidari, S.; Balaghi, S. E.; Holynska, M.; Sadr, M. H.; Soltani, B.; Khatamian, M.; Larkum, A. W.; Allakhverdiev, S. I., Proposed mechanisms for water

oxidation by Photosystem II and nanosized manganese oxides. *Biochim. Biophys. Acta* **2017,** *1858* (2), 156-174.

24. Schardt, B. C.; Hollander, F. J.; Hill, C. L., Isolation, Purification, and Characterization of High-Valent Complexes from a Manganese Porphyrin Based Catalytic Hydrocarbon Activation System - Crystal and Molecular-Structure of Mu-Oxo-Bis[Azido(Tetraphenylporphinato)Manganese(Iv)]. *J. Am. Chem. Soc.* **1982,** *104* (14), 3964-3972.

25. Schappacher, M.; Weiss, R., Formation of Manganese(Iv)-Oxo-Porphyrin Derivatives by Decomposition of Peroxycarbonate Complexes. *Inorg. Chem.* **1987,** *26* (8), 1189-1190.

26. Peng, Q. J.; Duan, Y. G.; Ouyang, Y. Z.; Fu, W. C., Regioselective oxidation of phenylethane with air catalyzed by mu-oxo-bis-manganese porphyrins. *Acta Chim. Sinica* **2001,** *17* (4), 292-294.

27. Song, W. J.; Seo, M. S.; George, S. D.; Ohta, T.; Song, R.; Kang, M. J.; Tosha, T.; Kitagawa, T.; Solomon, E. I.; Nam, W., Synthesis, characterization, and reactivities of manganese(V)-oxo porphyrin complexes. *J. Am. Chem. Soc.* **2007,** *129* (5), 1268-1277.

28. Lee, J. Y.; Lee, Y. M.; Kotani, H.; Nam, W.; Fukuzumi, S., High-valent manganese(v)-oxo porphyrin complexes in hydride transfer reactions. *Chem. Commun.* **2009,** (6), 704-706.

29. Fukuzumi, S.; Fujioka, N.; Kotani, H.; Ohkubo, K.; Lee, Y. M.; Nam, W., Mechanistic Insights into Hydride-Transfer and Electron-Transfer Reactions by a Manganese(IV)-Oxo Porphyrin Complex. *J. Am. Chem. Soc.* **2009,** *131* (47), 17127-17134.

30. Guo, M.; Dong, H.; Li, J.; Cheng, B.; Huang, Y. Q.; Feng, Y. Q.; Lei, A. W., Spectroscopic observation of iodosylarene metalloporphyrin adducts and manganese(V)-oxo porphyrin species in a cytochrome P450 analogue. *Nat. Commun.* **2012,** *3*.

31. Cannon, J. R.; Johnson, A. W.; Todd, A. R., Structure of Vitamin-B12 - a Crystalline Nucleotide-Free Degradation Product of Vitamin-B12. *Nature* **1954,** *174* (4443), 1168-1169.

32. Bonnett, R.; Cannon, J. R.; Johnson, A. W.; Sutherland, I.; Todd, A. R.; Smith, E. L., Structure of Vitamin-B12 and Its Hexacarboxylic Acid Degradation Product. *Nature* **1955,** *176* (4477), 328-330.

33. Nockolds, C. K.; Ramasesh.S; Hodgkin, D. C.; Waters, T. N. M.; Waters, J. M.; Moore, F. M.; Willis, B. T. M., Structure of a Monocarboxylic Acid Derivative of Vitamin B12. *Nature* **1967,** *214* (5084), 129-&.

34. Min, C. H.; Atshaves, B. P.; Roessner, C. A.; Stolowich, N. J.; Spencer, J. B.; Scott, A. I., Isolation, Structure, and Genetically-Engineered Synthesis of Precorrin-5, the Pentamethylated Intermediate of Vitamin-B12 Biosynthesis. *J. Am. Chem. Soc.* **1993,** *115* (22), 10380-10381.

35. Thibaut, D.; Debussche, L.; Frechet, D.; Herman, F.; Vuilhorgne, M.; Blanche, F., Biosynthesis of Vitamin-B12 - the Structure of Factor-Iv, the Oxidized Form of Precorrin-4. *J. Chem. Soc. Chem. Comm.* **1993,** (6), 513-515.

36. Krautler, B.; Konrat, R.; Stupperich, E.; Farber, G.; Gruber, K.; Kratky, C., Direct Evidence for the Conformational Deformation of the Corrin Ring by the Nucleotide Base in Vitamin-B12 - Synthesis and Solution Spectroscopic and Crystal-Structure Analysis of Co-Beta-Cyanoimidazolylcobamide. *Inorg. Chem.* **1994,** *33* (18), 4128-4139.

37. Ramdhanie, B.; Stern, C. L.; Goldberg, D. P., Synthesis of the first corrolazine: A new member of the porphyrinoid family. *J. Am. Chem. Soc.* **2001,** *123* (38), 9447-9448.

38. Ramdhanie, B.; Zakharov, L. N.; Rheingold, A. L.; Goldberg, D. P., Synthesis, structures, and properties of a series of four-, five-, and six-coordinate cobalt(III) triazacorrole complexes: The first examples of transition metal corrolazines. *Inorg. Chem.* **2002,** *41* (16), 4105-4107.

39. Kerber, W. D.; Goldberg, D. P., High-valent transition metal corrolazines. *J. Inorg. Biochem.* **2006,** *100* (4), 838-857.

40. Fox, J. P.; Ramdhanie, B.; Zareba, A. A.; Czernuszewicz, R. S.; Goldberg, D. P., Copper(III) and vanadium(IV)-Oxo corrolazines. *Inorg. Chem.* **2004,** *43* (21), 6600-6608.

41. Lansky, D. E.; Mandimutsira, B.; Ramdhanie, B.; Clausen, M.; Penner-Hahn, J.; Zvyagin, S. A.; Telser, J.; Krzystek, J.; Zhan, R. Q.; Ou, Z. P.; Kadish, K. M.; Zakharov, L.; Rheingold, A. L.; Goldberg, D. P., Synthesis, characterization, and physicochernical properties of manganese(III) and manganese(V)-oxo corrolazines. *Inorg. Chem.* **2005,** *44* (13), 4485-4498.

42. Cho, K.; Leeladee, P.; McGown, A. J.; DeBeer, S.; Goldberg, D. P., A High-Valent Iron-Oxo Corrolazine Activates C-H Bonds via Hydrogen-Atom Transfer. *J. Am. Chem. Soc.* **2012,** *134* (17), 7392-7399.

43. Goldberg, D. P., Corrolazines: New frontiers in high-valent metalloporphyrinoid stability and reactivity. *Acc. Chem. Res.* **2007,** *40* (7), 626-634.

44. Leeladee, P.; Jameson, G. N. L.; Siegler, M. A.; Kumar, D.; de Visser, S. P.; Goldberg, D. P., Generation of a High-Valent Iron Imido Corrolazine Complex and NR Group Transfer Reactivity. *Inorg. Chem.* **2013,** *52* (8), 4668-4682.

45. Mandimutsira, B. S.; Ramdhanie, B.; Todd, R. C.; Wang, H. L.; Zareba, A. A.; Czemuszewicz, R. S.; Goldberg, D. P., A stable manganese(V)-oxo corrolazine complex. *J. Am. Chem. Soc.* **2002,** *124* (51), 15170-15171.

46. Prokop, K. A.; Goldberg, D. P., Generation of an Isolable, Monomeric Manganese(V)-Oxo Complex from O-2 and Visible Light. *J. Am. Chem. Soc.* **2012,** *134* (19), 8014-8017.

47. Zaragoza, J. P. T.; Siegler, M. A.; Goldberg, D. P., A Reactive Manganese(IV)-Hydroxide Complex: A Missing Intermediate in Hydrogen Atom Transfer by High-Valent Metal-Oxo Porphyrinoid Compounds. *J. Am. Chem. Soc.* **2018,** *140* (12), 4380-4390.

48. McGuire, R.; Dogutan, D. K.; Shao-Horn, Y.; Nocera, D. G., Electrocatalytic oxygen reduction mediated by metalo-hangman-xanthene-porphyrin and -corrole complexes. *Abstr Pap Am Chem S* **2010,** *240*.

49. Dogutan, D. K.; McGuire, R.; Nocera, D. G., Electocatalytic Water Oxidation by Cobalt(III) Hangman beta-Octafluoro Corroles. *J. Am. Chem. Soc.* **2011,** *133* (24), 9178-9180.

50. Schwalbe, M.; Dogutan, D. K.; Stoian, S. A.; Teets, T. S.; Nocera, D. G., Xanthene-Modified and Hangman Iron Corroles. *Inorg. Chem.* **2011,** *50* (4), 1368-1377.

51. Dogutan, D. K.; Stoian, S. A.; McGuire, R.; Schwalbe, M.; Teets, T. S.; Nocera, D. G., Hangman Corroles: Efficient Synthesis and Oxygen Reaction Chemistry. *J. Am. Chem. Soc.* **2011,** *133* (1), 131-140.

52. Lai, W. Z.; Cao, R.; Dong, G.; Shaik, S.; Yao, J. N.; Chen, H., Why Is Cobalt the Best Transition Metal in Transition-Metal Hangman Corroles for O-O Bond Formation during Water Oxidation? *J. Phys. Chem. Lett.* **2012,** *3* (17), 2315-2319.

53. Graham, D. J.; Dogutan, D. K.; Schwalbe, M.; Nocera, D. G., Hangman effect on hydrogen peroxide dismutation by Fe(III) corroles. *Chem. Commun.* **2012,** *48* (35), 4175-4177.

54. Moser, F. H.; Thomas, A. L., *The Phthalocyanines*. CRC Press, Inc. : Boca Raton, Florida, 1983; Vol. I.

55. Leznoff, C. C.; Lever, A. B. P., *Phthalocyanines: Properties and Applications* VCH Publishers: New York, 1989.

56. Sorokin, A. B., Phthalocyanine Metal Complexes in Catalysis. *Chem. Rev.* **2013,** *113* (10), 8152-8191.

57. Meshitsuka, S.; Ichikawa, M.; Tamaru, K., Electrocatalysis by Metal Phthalocyanines in Reduction of Carbon-Dioxide. *J. Chem. Soc. Chem. Comm.* **1974,** (5), 158-159.

58. Kapusta, S.; Hackerman, N., Carbon-Dioxide Reduction at a Metal Phthalocyanine Catalyzed Carbon Electrode. *J. Electrochem. Soc.* **1984,** *131* (7), 1511-1514.

59. Zhang, A. J.; Zhang, W. M.; Lu, J. X.; Wallace, G. G.; Chen, J., Electrocatalytic Reduction of Carbon Dioxide by Cobalt-Phthalocyanine-Incorporated Polypyrrole. *Electrochem. Solid-State Lett.* **2009,** *12* (8), E17-E19.

60. Zhao, H. Z.; Zhang, Y.; Zhao, B.; Chang, Y. Y.; Li, Z. S., Electrochemical Reduction of Carbon Dioxide in an MFC-MEC System with a Layer-by-Layer Self-

Assembly Carbon Nanotube/Cobalt Phthalocyanine Modified Electrode. *Environ. Sci. Technol.* **2012,** *46* (9), 5198-5204.

61. Kusama, S.; Saito, T.; Hashiba, H.; Sakai, A.; Yotsuhashi, S., Crystalline Copper(II) Phthalocyanine Catalysts for Electrochemical Reduction of Carbon Dioxide in Aqueous Media. *ACS Catal.* **2017,** *7* (12), 8382-8385.

62. Zhu, Y.; Barat, R., Partial oxidation of methane over a ruthenium phthalocyanine catalyst. *Chem. Eng. Sci.* **2014,** *116*, 71-76.

63. Terao, R.; Nakazono, T.; Parent, A. R.; Sakai, K., Photochemical Water Oxidation Catalyzed by a Water-Soluble Copper Phthalocyanine Complex. *ChemPlusChem* **2016,** *81* (10), 1064-1067.

64. Broicher, C.; Artz, J.; Palkovits, S.; Antoni, H.; Drogeler, M.; Morales, D. M.; Stampfer, C.; Palkovits, R., Mesoporous manganese phthalocyanine-based materials for electrochemical water oxidation via tailored templating. *Catal. Sci. Technol.* **2018,** *8* (6), 1517-1521.

65. Jia, H. X.; Yao, Y. C.; Zhao, J. T.; Gao, Y. Y.; Luo, Z. L.; Du, P. W., A novel two-dimensional nickel phthalocyanine-based metal-organic framework for highly efficient water oxidation catalysis. *J. Mater. Chem.* **2018,** *6* (3), 1188-1195.

66. Atzori, M.; Tesi, L.; Morra, E.; Chiesa, M.; Sorace, L.; Sessoli, R., Room-Temperature Quantum Coherence and Rabi Oscillations in Vanadyl Phthalocyanine: Toward Multifunctional Molecular Spin Qubits. *J. Am. Chem. Soc.* **2016,** *138* (7), 2154-2157.

67. Ziolo, R. F.; Griffiths, C. H.; Troup, J. M., Crystal-Structure of Vanadyl Phthalocyanine, Phase-Ii. *J. Chem. Soc. Dalton Trans.* **1980,** (11), 2300-2302.

68. Morawski, O.; Izdebska, K.; Karpiuk, E.; Suchocki, A.; Zhydachevskyy, Y.; Sobolewski, A. L., Titanyl Phthalocyanine as a Water Photooxidation Agent. *J. Phys. Chem. C* **2015,** *119* (25), 14085-14093.

69. Seikel, E.; Grau, M.; Kasmarker, R.; Oelkers, B.; Sundermeyer, J., Synthesis and crystal structure of novel, soluble titanyl phthalocyanines. *Inorg. Chim. Acta* **2011,** *374* (1), 119-126.

70. Hunt, C. C.; Peterson, M.; Anderson, C.; Wu, G.; Scheiner, S.; Sepunaru, L.; Ménard, G., Manuscript in preparation

71. Zhou, W.; Thompson, J. R.; Leznoff, C. C.; Leznoff, D. B., The Redox-Active Chromium Phthalocyanine System: Isolation of Five Oxidation States from (Pc4-CrI) to (Pc2-CrIII). *Chen, Eur. J.* **2017,** *23* (10), 2323-2331.

72. Sorokin, A. B.; Kudrik, E. V.; Bouchu, D., Bio-inspired oxidation of methane in water catalyzed by N-bridged diiron phthalocyanine complex. *Chem. Commun.* **2008,** (22), 2562-2564.

73. Kudrik, E. V.; Sorokin, A. B., N-bridged diiron phthalocyanine catalyzes oxidation of benzene with H2O2 via benzene oxide with NIH shift evidenced by using 1,3,5-[D-3]benzene as a probe. *Chen, Eur. J.* **2008,** *14* (24), 7123-7126.

74. Kudrik, E. V.; Afanasiev, P.; Bouchu, D.; Millet, J. M. M.; Sorokin, A. B., Diiron N-bridged species bearing phthalocyanine ligand catalyzes oxidation of methane, propane and benzene under mild conditions. *J.Porphyrins Phthalocyanines* **2008,** *12* (10), 1078-1089.

75. Afanasiev, P.; Bouchu, D.; Kudrik, E. V.; Millet, J. M. M.; Sorokin, A. B., Stable N-bridged diiron (IV) phthalocyanine cation radical complexes: synthesis and properties. *Dalton Trans.* **2009,** (44), 9828-9836.

76. Colomban, C.; Kudrik, E. V.; Afanasiev, P.; Sorokin, A. B., Catalytic Defluorination of Perfluorinated Aromatics under Oxidative Conditions Using N-Bridged Diiron Phthalocyanine. *J. Am. Chem. Soc.* **2014,** *136* (32), 11321-11330.

77. Colomban, C.; Kudrik, E. V.; Briois, V.; Shwarbrick, J. C.; Sorokin, A. B.; Afanasiev, P., X-ray Absorption and Emission Spectroscopies of X-Bridged Diiron Phthalocyanine Complexes (FePc)(2)X (X = C, N, O) Combined with DFT Study of (FePc)(2)X and Their High-Valent Diiron Oxo Complexes. *Inorg. Chem.* **2014,** *53* (21), 11517-11530.

78. Afanasiev, P.; Sorokin, A. B., mu-Nitrido Diiron Macrocyclic Platform: Particular Structure for Particular Catalysis. *Acc. Chem. Res.* **2016,** *49* (4), 583-593.

Chapter 2: Synthesis and Characterization of Substituted Phthalocyanines

2.1 Introduction

The first metal-free phthalocyanine was accidentally synthesized in 1907 as a byproduct in the synthesis of 2-cyanobenzamide. Two decades later the first metallated phthalocyanine was synthesized from 1,2-dibromobenzene in the presence of copper(I) cyanide. In this process, phthalonitrile is formed as an intermediate and followed by cyclotetramerization to form a copper phthalocyanine. After this discovery, Linstead and coworkers synthesized a number of metallophthalocyanines. Initially, the newly discovered copper phthalocyanines in particular were used as pigments, but their use has since expanded to include a number of chemical transformations as catalysts.[1]

Phthalocyanines have been made through a number of different syntheses and precursors. All are synthesized through a templated synthetic route using a precursor such as an (**Figure 2.1a**) isoindoline-1,3-diimine, (**Figure 2.1b**) phthalic acid, (**Figure 2.1c**) phthalamide, (**Figure 2.1d**) isoindoline-1,3-dione, (**Figure 2.1e**) 2-cyanobenzamide, or (**Figure 2.1f**) phthalonitrile. A metal species acts as the template for these precursors to form a tetracycle surrounding the metal center.[3, 7-12] In some instances, a base such as 1,8-diazabicyclo(5.4.0)undec-7-ene (DBU) is used in addition to the metal salt to aid in the synthesis of a phthalocyanine species.[13]

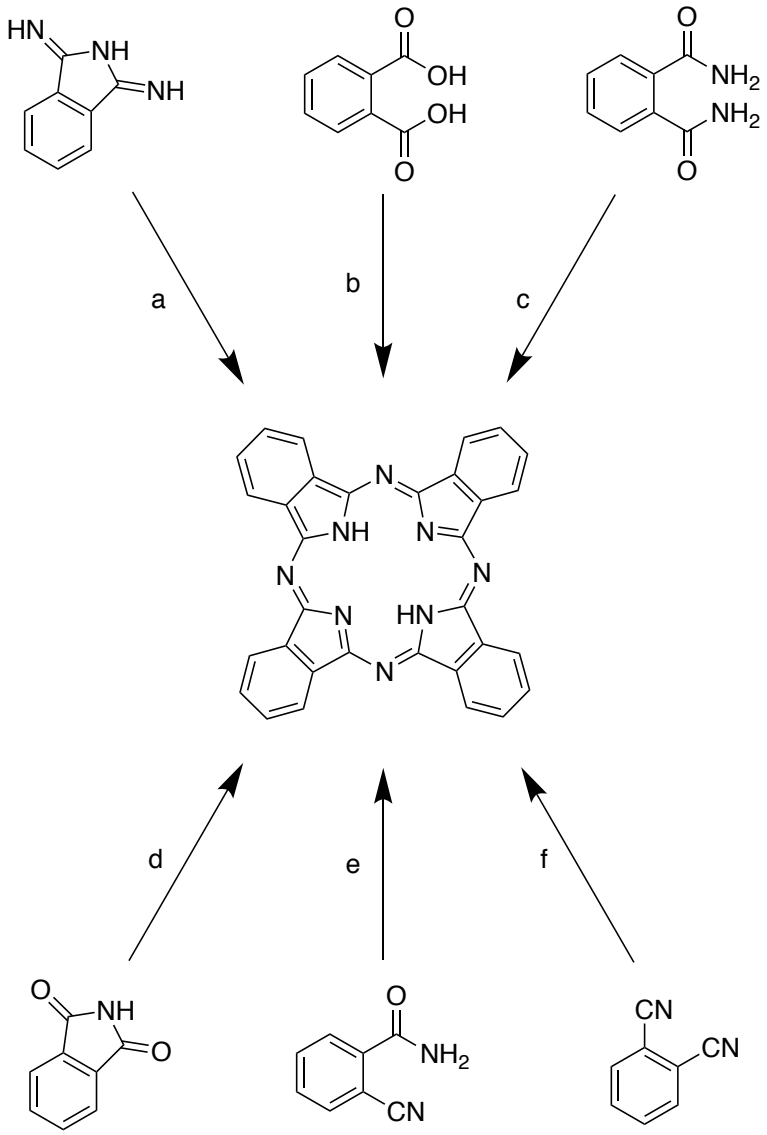

Figure 2.1. These are six precursors that all can be used to synthesize a phthalocyanine species. Each of these is capable of cyclotetramerization in order to form a phthalocyanine.[2-6]

Unsubtituted phthalocyanines are often found to be poorly soluble in organic solvents and aqueous media. Their planar shape, as well as extended π structure often leads to extensive stacking both in the solid and solution phases, thereby severely limiting their solubility.[14-15] Substitutions can make the phthalocyanine more soluble, but come with their own challenges. When there is a single substitution on the phthalocyanine, it is

possible to get four different regioisomers (**Figure 2.2**). During macrocycle synthesis, there is no controlling the regioselectivity of the reaction so multiple regioisomers can form. This requires additional work in order to isolate a single isomer.[16]

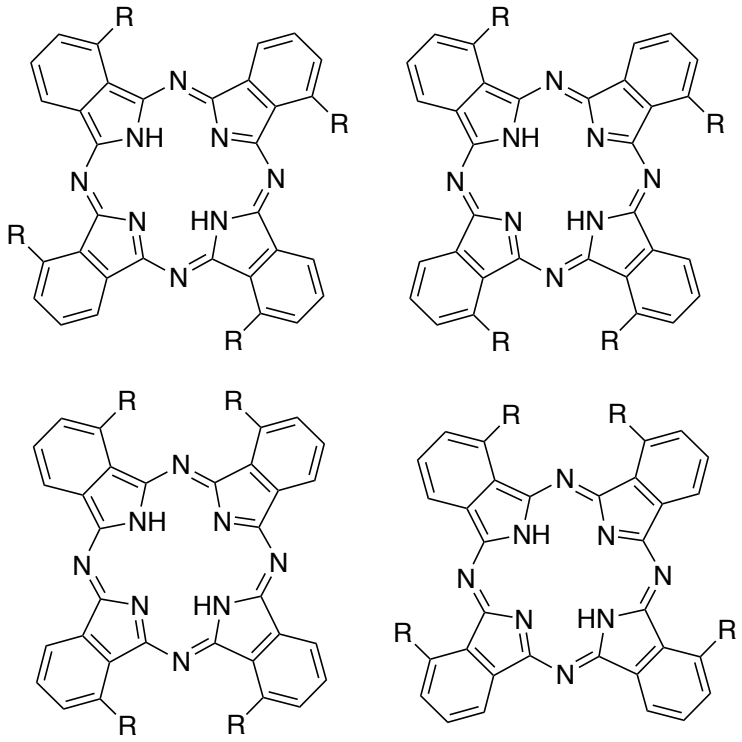

Figure 2.2. Possible regioisomers for a tetrakis- substituted phthalocyanine.

Alternatively, symmetrically substituted starting materials result in the isolation of a single product.[17] Rauchfuss previously synthesized a phthalocyanine ligand containing both isopropoxy and ethoxy-substituted phthalocyanines (**Figure 2.3**). These phthalocyanines were synthesized in order to study their functionality as π ligands. This group wished to see where a cationic ruthenium(II) pentamethylcyclopentadienyl species would bind since phthalocyanines contain a π system in both their pyrrole rings and their benzene rings.[8] These ligands are synthesized from a symmetric phthalonitrile. This eliminates the potential of additional products as there is no issues with regioisomers. In addition, this aids in the solubiliy of the phthalocyanine species.

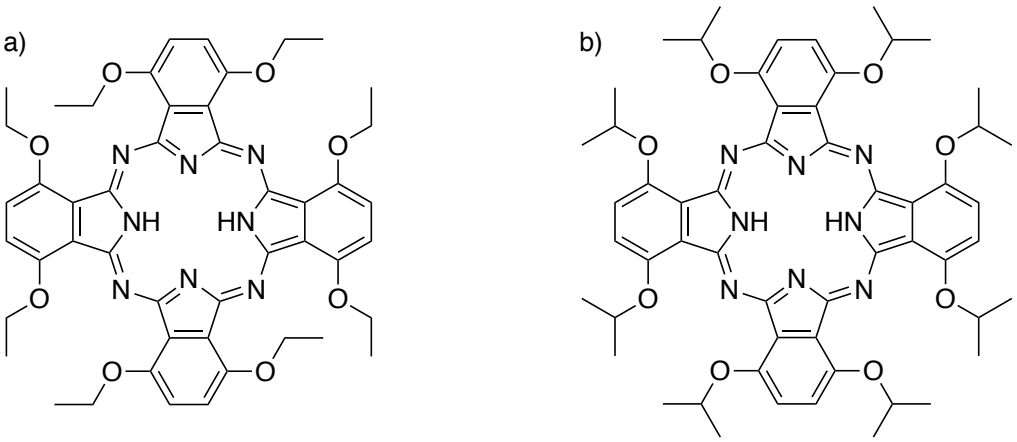

Figure 2.3. Structures of a) octaethoxy substituted phthalocyanine and b) octaisopropoxy substituted phthalocyanine.

Literature has shown pathways to metallated octaethoxy- and octaisopropoxy-substituted phthalocyanines. Previously, syntheses of manganese, nickel, copper, and vanadium (vandayl) octaethoxy phthalocyanines have been published.[8, 18] With the ultimate goal of forming a terminal metal oxo phthalocyanine species, knowledge of a synthetic pathway to a vanadyl phthalocyanine was useful in forming a terminal oxo species. Similarly, the ability of manganese to form a terminal nitride made it a metal of interest. Chromium should be quite similar in molecular orbital structure as it is situated between these species on the periodic table. When looking at the molecular orbital structure of early transition metals compared with later transition metals, the d orbitals are higher in energy for earlier transition metals. [19-21] Advancing towards the later transition metals in the periodic table, more electrons are added to the d-orbitals making it even less likely that a terminal species forms. This limited the metals of study to vanadium, chromium, and manganese as two of the three have already shown promise toward the goal of oxo formation, which will be elaborated on in Chapter 3.

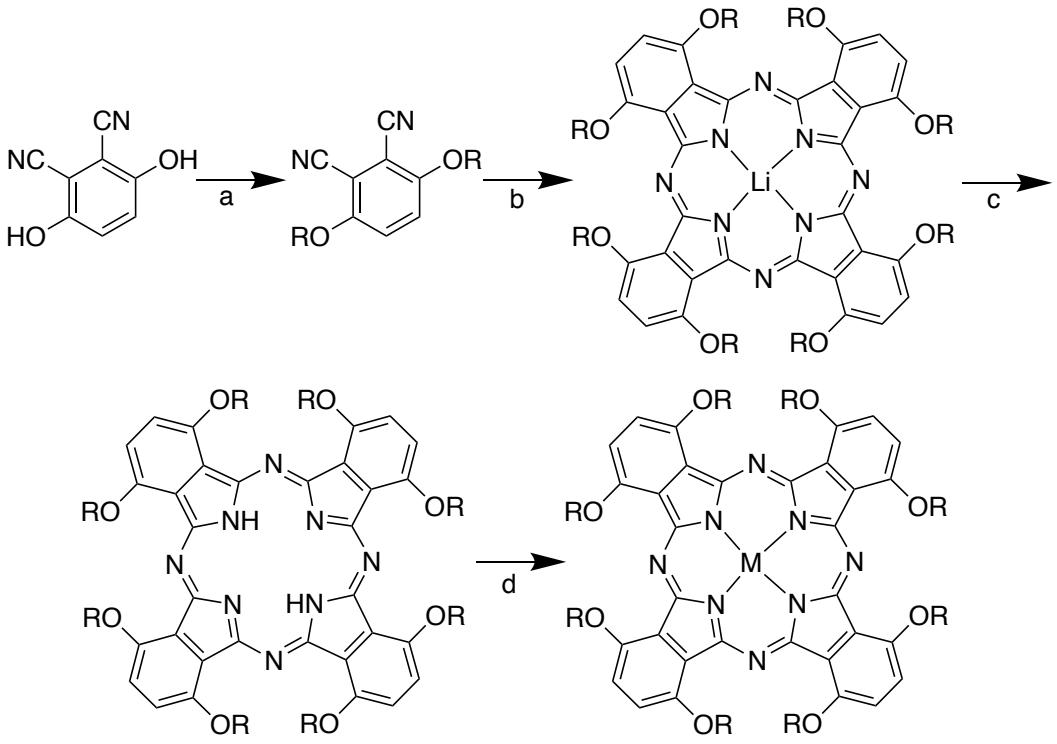

Figure 2.4. General schematic of phthalocyanine synthesis. (a) Acetone, iodoethane, reflux, 72 h, 63% yield (b) Ethanol, lithium, 5 d, 90% yield (c) 1:1 water/ethanol, HCl, 48 h, 81% yield (d) DMF or THF, $M(X)_2$, 2-5 h, 77-86% yield

In this chapter the synthesis of ethoxy and isopropoxy phthalocyanine ligands is discussed. The synthesis and characterization of chromium and manganese phthalocyanine species will also be described. The reactivity of these species will be discussed in the following chapter (**Figure 2.4**).

2.2 Results and Discussion

2.2.1 Ethoxy Phthalonitrile Synthesis and Characterization (2.1)

The synthesis of our 3,6-diethoxyphthalonitrile was optimized from the reported Rauchfuss literature procedure.[8] Addition of an excess of 2 equivalents iodoethane to a refluxing solution of 2,3-dicyanohydroquinone and potassium carbonate in acetone yields

a white powdery precipitate (**Scheme 2.1**). Once the solution is filtered and washed with water, ethanol, and ether, the solid is dried under vacuum to afford a 63% yield of the product (**1**).

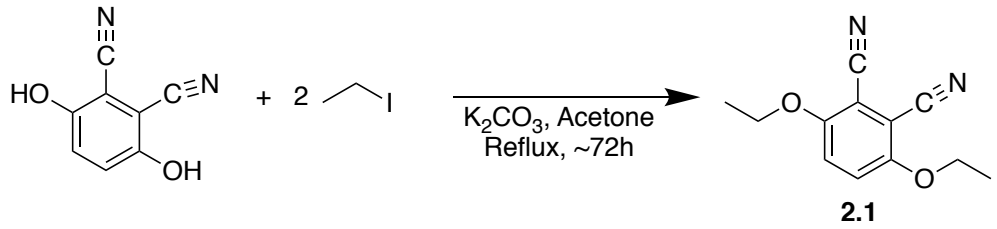

Scheme 2.1. Synthesis of **2.1**.

The ^{1}H NMR spectrum of the species in $CDCl_3$ exhibits one signal in the phenyl region at 7.14 ppm corresponding to the phenyl proton of the species. There are an additional two resonances observed at 4.13 ppm (quartet) and 1.47 ppm (triplet), assigned to the methylene and methyl groups, respectively.

2.2.2 Lithiated Phthalocyanine Synthesis and Characterization (2.2)

The cyclization of **2.1** into a phthalocyanine was optimized from the reported synthesis.[8] A large excess of lithium pellets was added to a slurry of precursor in refluxing ethanol. After several hours, the solution turned a deep evergreen color. The solution was heated for five days, after which it was filtered to afford a pure green solid (**2**) in 90% yield (**Scheme 2.2**).

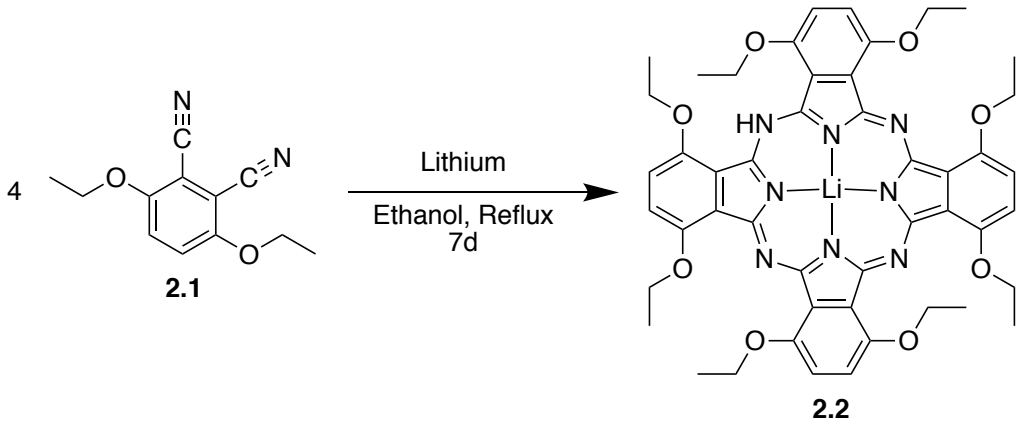

Scheme 2.2. Synthesis of **2.2**.

The ^{1}H NMR spectrum of this species reveals four representative resonances in $CDCl_3$. The spectrum exhibits complicated splitting patterns as the lithium is not completely centralized in the center of the phthalocyanine. This causes all of the signals in the ^{1}H NMR to have slightly different shifts so that there are multiple peaks, representative of the protons in the phthalocyanine. There is a series of singlets at approximately 7.47 ppm that are representative of the phenyl protons in the phthalocyanine. There are a series of overlapping quartets at 4.93 ppm and a series of overlapping triplets at 1.83 ppm that are representative of the ethoxy groups on the phthalocyanine. Lastly there is a downfield shifted proton at 14.73 ppm. This signal is representative of a proton bound to one of the nitrogen atoms. The far downfield shift is a result of ring current. As the magnetic field of the NMR is directed perpendicular to the plane of the phthalocyanine ring, it induces a magnetic field to be formed in the freely circulating π-electrons of the phthalocyanine ring. Protons on the exterior of the ring experience further deshielding as the magnetic fields of both the NMR and the induced magnetic field are aligned. This shifts the signals further downfield. Alternatively, a proton from within the field would be shifted further upfield as it experiences shielding from both fields being in opposite directions.[22-24]A ^{7}Li NMR spectrum was collected on **2** in order to confirm the presence of a lithium atom in the phthalocyanine. In $CDCl_3$ the lithium signal was seen at -8.47 ppm.

In order to further confirm the composition of **2.2**, we performed mass spectrometry (MS) on the compound. Compound **2.2** was subjected to matrix assisted laser desorption/ionization-time of flight (MALDI-TOF), and the mass spectrum

confirmed that the crude product is a mixture of both lithiated and protonated phthalocyanines. Signals in the MALDI-TOF at both 866.5 m/z and 872.5 m/z, consistent with the protonated form of octaethoxyphthalocyanine species **(2.3)** and the lithiated form of the octaethoxyphthalocyanine **(2.2)** respectively.

2.2.3 Protonated Phthalocyanine Synthesis and Characterization (2.3)

In order to generate a clean, uniform Pc, we treated the crude product (**Scheme 2.2**) to acid in order to remove the lithium (**Scheme 2.3**). Hydrochloric acid was added to a solution of the lithiated product in a 1:1 water:ethanol solvent system. This caused the green product to turn a purplish-blue color. After heating to 45 ^{o}C for 48 h the solution was neutralized then filtered. The isolated green product was dried to yield 81.3% of pure product **2.3** (**Scheme 2.3**). Care must be taken as excessive heating of the acidic solution resulted in breakdown of the Pc structure to the starting monomer. Monitoring the reaction daily by ^{1}H NMR spectroscopy was therefore performed in order to avoid this decomposition pathway.

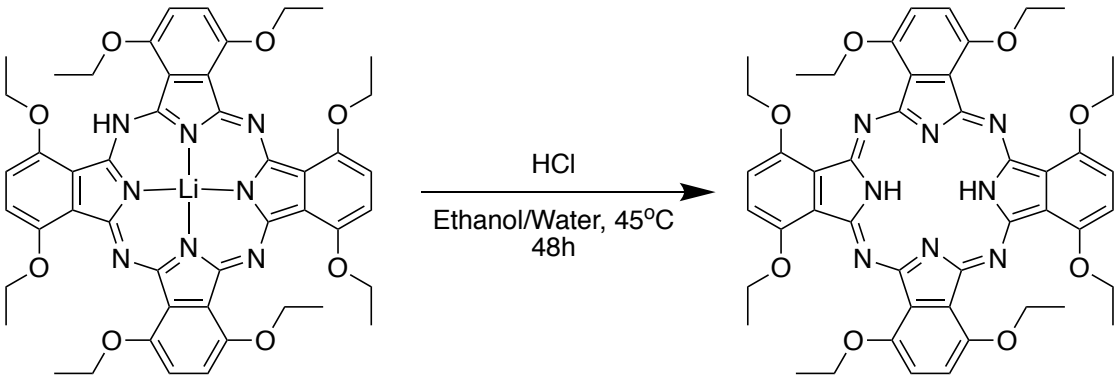

Scheme 2.3. Synthesis of **2.3**.

The ^{1}H NMR spectrum of **3** in $CDCl_3$ shows four clear signals, confirming the removal of lithium. The first signal of these is the singlet at 7.60 ppm which is

representative of the phenyl protons. There are two signals that represent the ethoxy linker, a quartet centered at 4.95 ppm and a triplet centered at 1.84 ppm. Finally, there is a singlet at 0.20 ppm, which represents the N–H protons. In addition, the disappearance of the singlet at 14.73 ppm is a good indication that the lithiated species has been removed. As previously stated, ring current accounts for the upfield shift of the N-H proton and confirms that the protonated form of the ligand is isolated. In contrast to the mixture above **2.2**, the MALDI-TOF spectrum of **2.3** confirmed the clean conversion observed by the disappearance of the peak at 872.5 m/z, and a clean peak at 866.5 m/z, consistent with product formation.

Single crystals suitable for X-ray diffraction (XRD) studies were grown from dichloromethane (DCM) and diethyl ether by vapor diffusion, to yield hexagonal green plates. The solid-state structure of **2.3** was obtained and is shown in **Figure 2.5**. The structure of highly substituted phthalocyanines tend to form a saddle shape. This is due to strong repulsive interactions between atoms in the substitutions that cause the structure to twist.[25-26] In the pyrrole rings of **2.3** the C-$N_{pyrrole}$, bonds have lengths between 1.360-1.385Å, while in the linkers the C-N_{linker} bonds are between 1.311-1.352 Å. In unsubstituted phthalocyanines, the C-$N_{pyrrole}$ length averages between 1.36-1.37 Å, which is comparable to the 1.360-1.285 Å lengths seen in the ethoxy substituted complex. The C-N_{linker} bonds are seen to be 1.27-1.30 Å, which is shorter then the bond lengths of 1.311-1.352 Å in **2.3**.[27] This is likely due to the substituents causing the ring to twist and become saddle shaped.

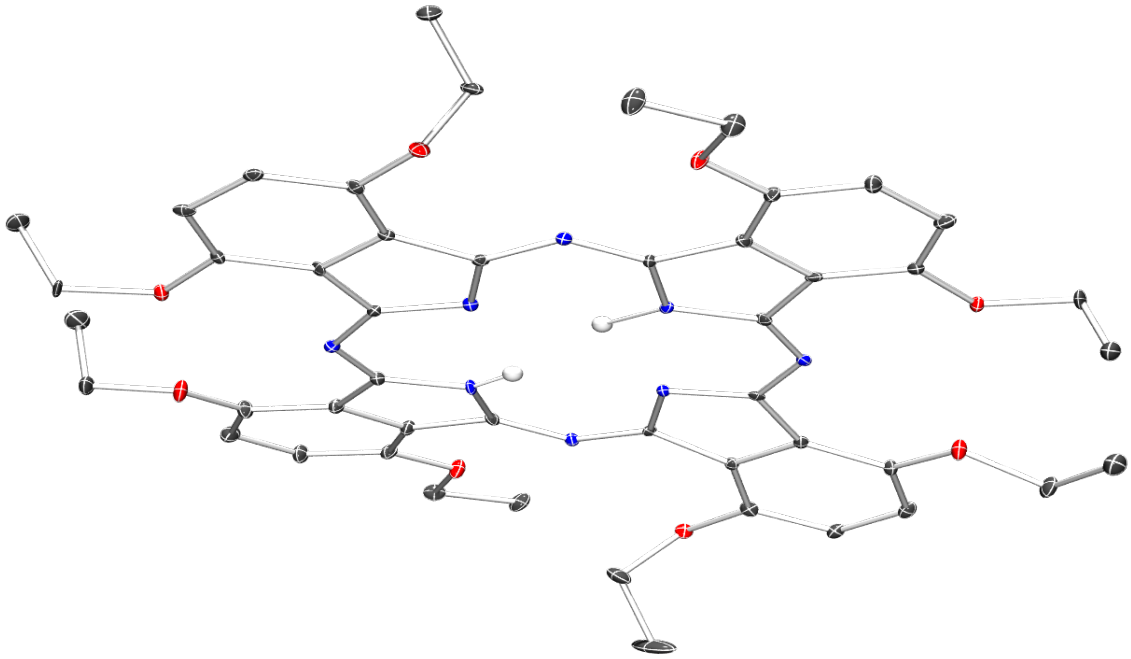

Figure 2.5. Solid-state crystal structure of **2.3.** H atoms, except N-H, are removed for clarity. Selected bond lengths (Å): N-H 0.880-0.894, C-$N_{pyrrole}$ 1.360(6)-1.385(6), C-N_{linker} 1.311(7)-1.352(6).

2.2.4 Chromium(II) Phthalocyanine Synthesis and Characterization (2.4)

Attempts to make a chromium(II) phthalocyanine using previously reported methods proved to be unsuccessful in generating and cleanly isolating the desired product. In order to synthesize the chromium(II) phthalocyanine, a new strategy that has not been employed to other phthalocyanine species was attempted. Using acid-base chemistry, compound **2.3** was reacted with the basic species, $Cr(N(SiMe_3)_2)_2{\cdot}THF_2$, in tetrahydrofuran (THF) solvent (**Scheme 2.4**).[28-29] Using hexamethylbenzene as an internal standard, the ^{1}H NMR spectrum revealed the formation of $HN(SiMe_3)_2$ with complete conversion occurring after 2.5 hours. The product was washed with hexanes, water, and ethanol and subsequently dried under vacuum to produce a blue-green powder in 86% yield.

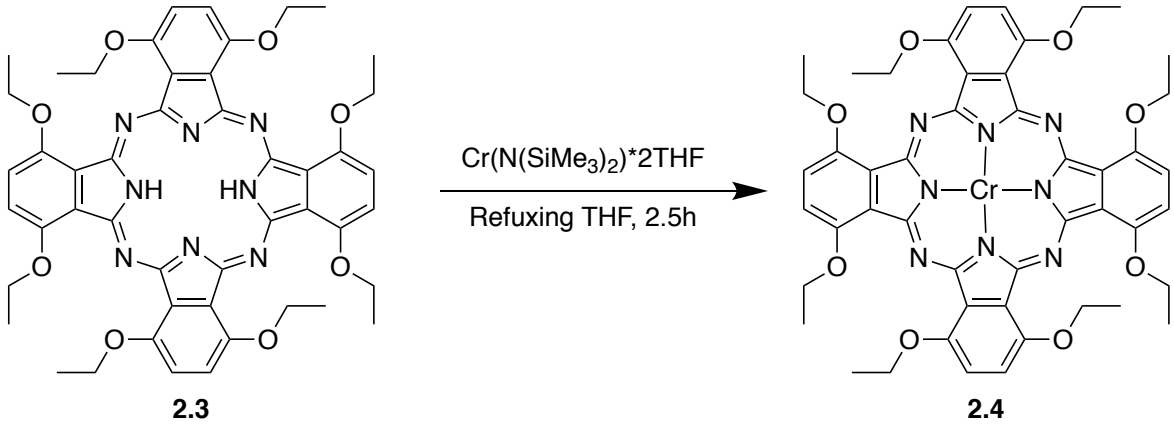

2.3 **2.4**

Scheme 2.4. Synthesis of **2.4**.

The MS of **2.4** was collected using both electron-spray ionization (ESI) and MALDI-TOF methods in order to confirm the identity of the blue-green species. In MALDI-TOF the molecular ion of [M+] was found at 916.460 m/z. In the ESI the [M+] was found to be 1060.4 m/z. The former corresponds to the mass of **2.4** while the latter corresponds to the molecular weight of **2.4** with two molecules of THF coordinated to it.

The ^{1}H NMR spectrum of **2.4** in $CDCl_3$ was taken and gives a spectrum of broadened signals. There are two broadened signals visible located at 1.86 ppm and 3.94 ppm. These signals do not integrate to give us a clear idea of which protons they represent, however, a similar trend is seen with other metal phthalocyanines synthesized such as the cupric and the vanadyl phthalocyanine species isolated by Rauchfuss.[8]

Single crystals of **2.4** suitable for XRD studies were grown from DCM and diethyl ether to yield green plates. When grown, the refined structure appears to contain water coordinated to the chromium center on both axial positions of the atom (**Figure 2.6**). The structure retains some is saddle shape with chromium bound in the center. The metal is centralized in the pocket of the phthalocyanine and does not pucker out of the ring. This is very similar to the unsubstituted phthalocyanine isolated by Leznoff. The

unsubstituted phthalocyanine isolated by Leznoff has coordinated THF with Cr-O_{THF} bond lengths of 2.053(3) Å. The Cr-O_{Water} bond length is elongated in the isolated refined structure having a bond length of 1.995(3) Å. The Cr-N bond lengths seen in the unsubstituted phthalocyanine have bond lengths of 1.968(6) Å and 1.982(5) Å.[9] In **2.4** the bond lengths are seen as 1.987(4) Å and 1.984(4) Å. The substitutions and their twisting of the ring causes these lengths to be elongated slightly as can be seen from the comparisons of **2.3** to unsubstituted phthalocyanines.

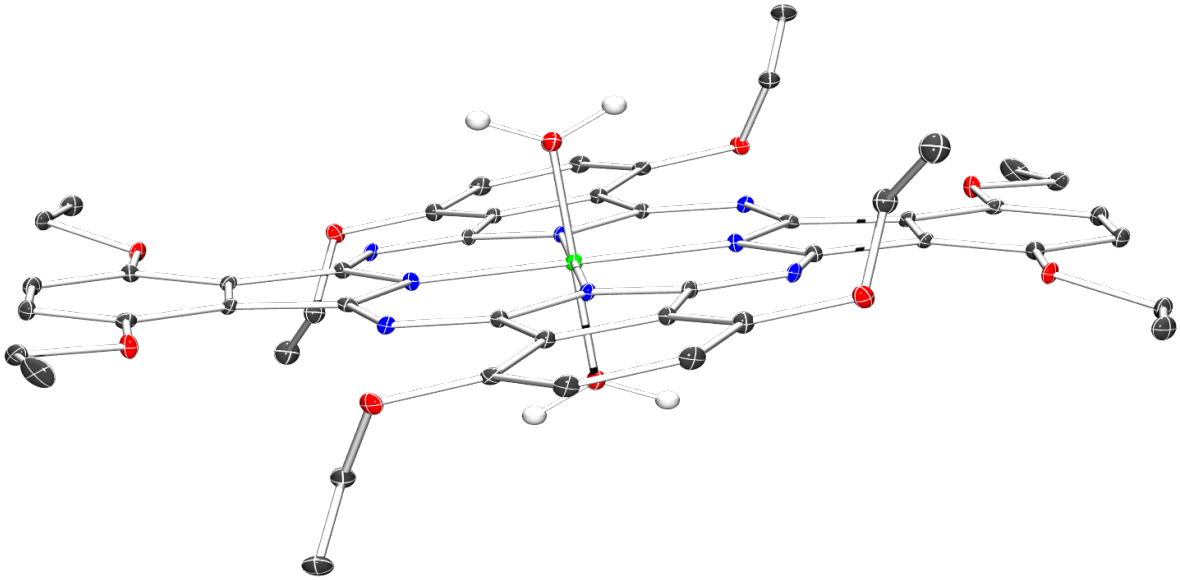

Figure 2.6. Crystal structure of **2.4**. Protons removed for clarity, except for H_2O. Selected bond lengths (Å): Cr-O_{Water}: 1.995(3), Cr-N_1: 1.987(4) Cr-N_2: 1.984(4)

2.2.5 Manganese Chloride(III) Phthalocyanine Synthesis and Characterization (2.5)

The manganese phthalocyanine was synthesized by addition of five equivalents of manganese(II) chloride and five equivalents of potassium bicarbonate to a solution of **2.3** in refluxing dimethylformamide (DMF) in open air, yielding a reddish solution after 5 hours. Water is added to this solution and the product precipitates out on cooling

overnight. The red powder is filtered off and dried under vacuum resulting in a 77% yield of pure product, **2.5** (**Scheme 2.5**).

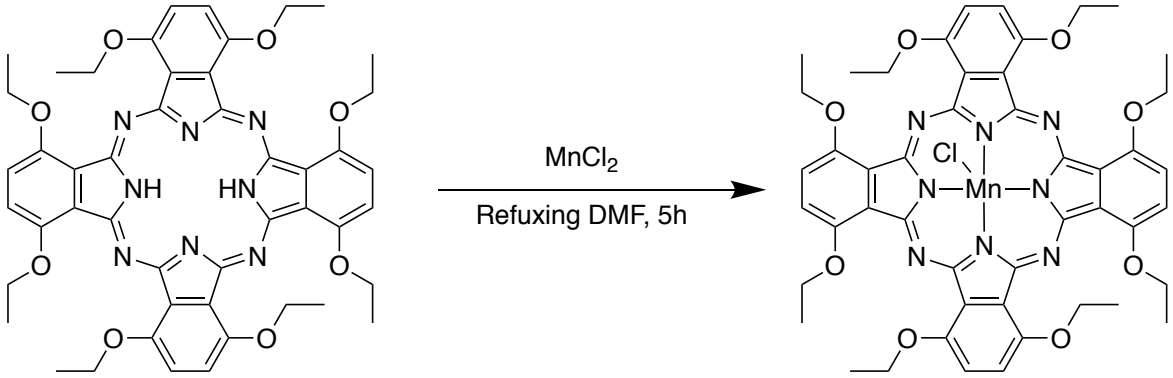

2.3 **2.5**

Scheme 2.5. Synthesis of **2.5**

The ^{1}H NMR spectrum of this species in CD_2Cl_2 yields paramagnetically shifted resonances at 6.72 ppm, 1.83 ppm, and -5.79 ppm. The peaks are significantly broadened and difficult to integrate due to the paramagnetism rendering them unassignable. The MS of **2.5** was collected by MALDI-TOF. The spectrum revealed a molecular ion peak at 954.805 m/z, consistent with the structure of **2.5**. In addition, a peak is seen in the mass spectrum with a value of 919.835 m/z. This peak corresponds to the manganese species without the axial chloride ion.

Single crystals of **2.5** suitable for XRD studies for the structure below can be grown from DCM and diethyl ether to yield red crystals. The refined structure of **2.5** has a saddle shape similarly to the other isolated phthtalocyanine species isolated (**Figure 2.7**). Mn-Cl: 2.379(3) Å, Mn-N_1: 1.968(8) Å, Mn-N_2: 1.954(8) Å; Mn-N_3: 1.950(8) Å; Mn-N_4: 1.960(7) Å. When compared with a porphyrin system these bond lengths are similar, though shorter in comparison. The porphyrin system has a Mn-Cl bond length of 2.4325(7) Å which, though longer than the 2.379(3) Å seen in **2.5,** is comparable to that

of the phthalocyanine. This could be a result of water coordination to make an octahedral environment around the porphyrin. The porphyrin Mn-N bond lengths range from 2.0160 to 2.0275(19) Å where as the phthalocyanine has bond lengths that are shorter, with a range of 1.950(8)- 1.968(8) Å. Again this shorter bond length is due to some slight differences in the structure of the phthalocyanine and porphyrin ligands.[30]

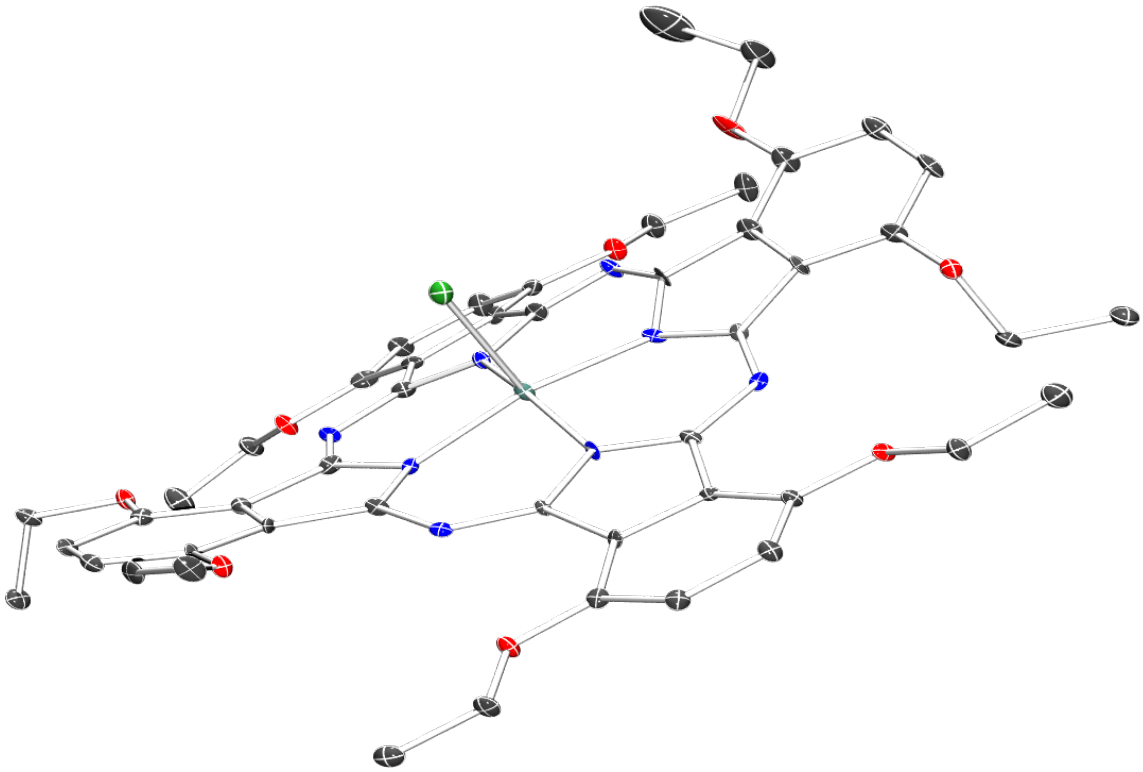

Figure 2.7. Crystal structure of **2.5**. Protons removed for clarity. Selected bond lengths (Å): Mn-Cl: 2.379(3), Mn-N_1:1.968(8), Mn-N_2: 1.954(8)Mn-N_3:1.950(8), Mn-N_4:1.960(7)

2.2.6 "Naked" Manganese (III) Phthalocyanine Synthesis and Characterization (2.6)

Looking toward the goal of obtaining a manganese oxo species, we first sought to remove the chloride from the axial position of the Mn center. A lot of success has been seen with coordinatively unsaturated Mn(III) corrole species synthesized by the Goldberg

group, and we wished to try and mimic their species. Their corrole ligand has a -3 charge and therefore they use a manganese(III) species to fill their pocket. O-atom donors are then used to create the oxo (**Scheme 1.2**). In order to generate a coordinatively unsaturated version of **2.5**, we exposed it to the silylium cation, $[Et_3Si][B(C_6F_5)_4]$,[31] dissolved in benzene.[32] Upon addition, the red solution of **2.5** turns a blue-green and precipitation occurs. The benzene is decanted to isolate the blue solid (**Scheme 2.6**).

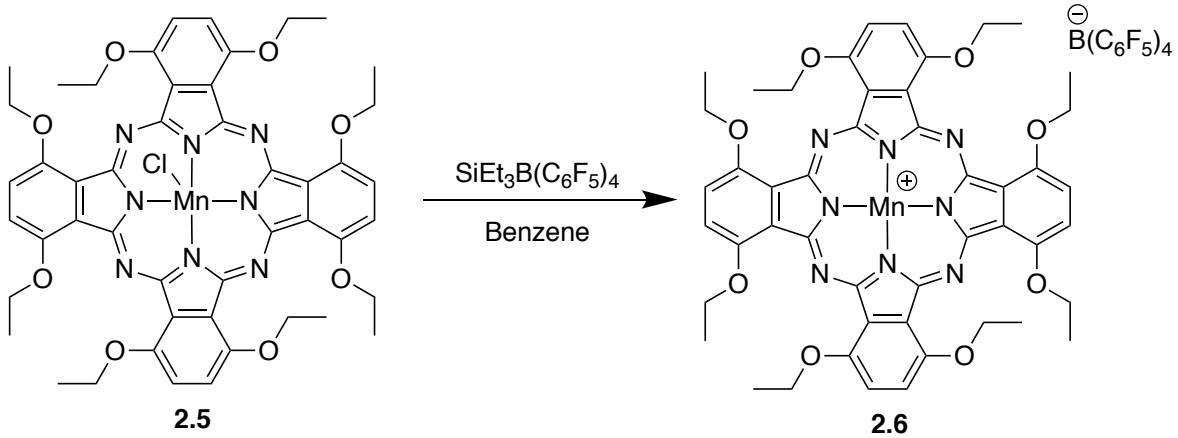

2.5 **2.6**

Scheme 2.6. Synthesis of **2.6**.

When the reaction is done on an NMR scale in d_6-benzene, the ^{1}H NMR of the solution yields two signals. The two signals appear at 0.51 ppm and 0.96 ppm. The signal at 0.96 ppm is a quartet and the signal at 0.51ppm is a triplet. These species represent the CH_2 and CH_3 in the ethyl groups branching off of the silicon atom. In addition ^{11}B NMR is run and there is an absence of signal. The ^{19}F NMR spectrum is also silent. This all corresponds to the formation of chlorotriethyl silane and the "naked" manganese species. The "naked" manganese species is the insoluble crude product.

The crude blue solid of **2.6** can be dissolved in coordinating solvents such as acetonitrile and THF. When dissolved in d_3-acetonitrile, the ^{1}H NMR spectrum was

silent. The one single in the ^{11}B NMR spectrum is at -16.63 ppm corresponding to the $[B(C_6F_5)_4]^-$ anion. The ^{19}F NMR spectrum contains three signals for the *ortho*, *para*, and *meta* fluorines of the aryl groups. The *meta* fluorine resonance is at -133.66 ppm, while the *para* and *ortho* fluorines are at -163.97 ppm and -168.34 ppm, respectively. These are all in accordance with the $[B(C_6F_5)_4]^-$ counterion.

Complex **2.6** was also analyzed by ESI MS in acetonitrile. No evidence of the chlorinated species is seen and two signals are shown suggesting the existence of **2.6**. One signal at 919 m/z corresponds to the manganese(III) stripped of the chlorine atom. In addition, there is a signal at 960.3m/z, which corresponds to the species with a coordinated acetonitrile. No species is seen however with two molecules of acetonitrile coordinated. This is surprising as there are two axial positions for the coordination of acetonitrile and the coordination of two molecules of solvent has already been seen in the chromium species, with THF coordination.

2.2.7 Isopropoxy Phthalonitrile Synthesis and Characterization (2.7)

The synthesis of our 3,6-diethoxyphthalonitrile was optimized from the reported Rauchfuss literature procedure.[8] The synthesis of the 3,6-diisopropylphthalonitrile is very similar to the ethoxy-substituted phthalonitrile. Five equivalents of 2-iodopropane was added to a solution of 2,3-dicyanoquinone and potassium carbonate in acetone. After refluxing for 72 hours, the reaction was pulled and the solid was filtered off. The solid was washed with acetone and water was added to the mother liquor to precipitate the solid product. The product is filtered off to give a white solid powder. The product is dried under vacuum with a yield of 51% (**Scheme 2.7**).

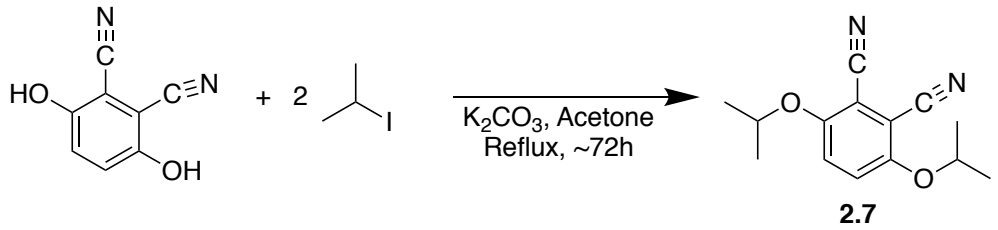

2.7

Scheme 2.7. Synthesis of **2.7**

The ^{1}H NMR spectrum of **2.7** was taken in $CDCl_3$ and afforded three resonances. There is a signal at 7.15 ppm in the aromatic region representative of the two aryl protons. There is also a septet centered at 4.57 ppm and a doublet at 1.39 ppm representative of the isopropyl group.

Single crystals are grown from DCM and diethyl ether to yield white needles. These diffract to show the below structure confirming our synthesis (**Figure 2.8**). The C-N bond lengths of 1.141 Å are comparable to other C-N bond lengths in other phthalonitriles where the bond lengths tend to be 1.140 and 1.142 Å. In addition, the ether lengths compare for other substituted phthalonitriles, with ethereal bonds. The C_{Ph}-O bond lengths are between 1.3633-1.3719 Å and the C-O 1.400-1.4057 Å, where the phthalonitrile synthesized has bond lengths of 1.357 and 1.456 Å respectively. The second length is slightly longer, but comparable with the different ether complexes.[33]

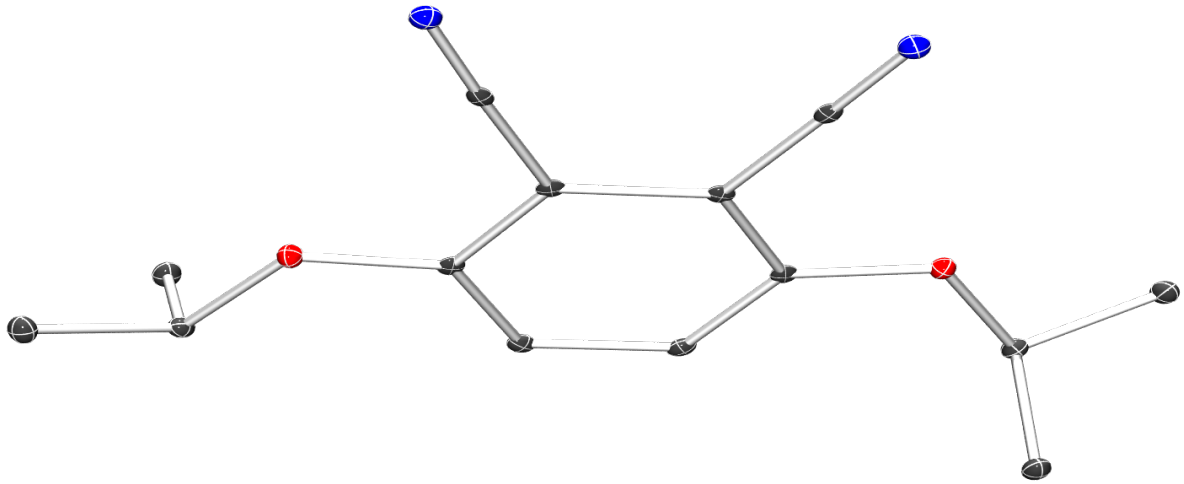

Figure 2.8. Crystal structure of **2.7**. Protons removed for clarity. Selected bond lengths (Å): C-N:1.144(3), C_{Ph}-O: 1.357(2), 1.456(2)

2.2.8 Isopropoxy Phthalocyanine Synthesis and Characterization (2.8 and 2.9)

The synthesis of the isopropoxy-substituted phthalocyanine was optimized from a synthesis previously reported by Rauchfuss. A slurry of the precursor in isopropyl alcohol is treated with excess lithium. On treatment the solution begins to turn a blue green color which darkens over time. The solution was heated to reflux for 72 hours after which time the reaction is cooled and filtered to yield a green powder product (**Scheme 2.8**).

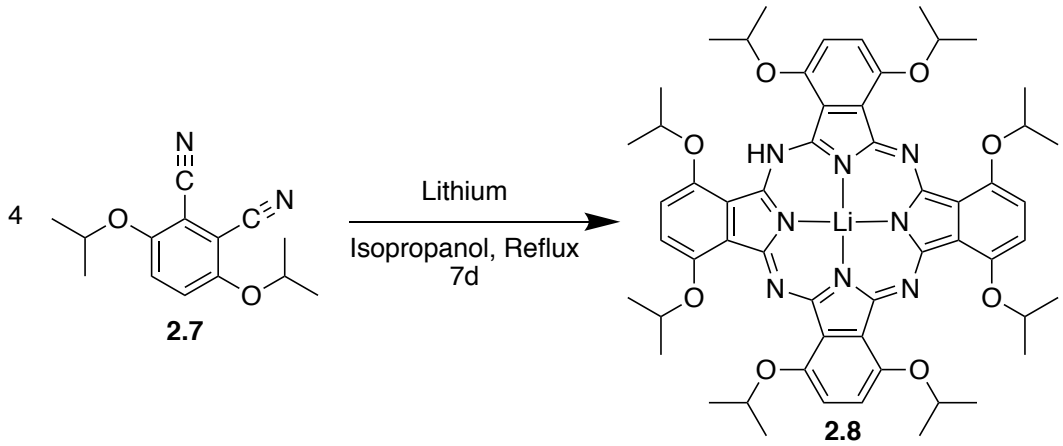

Scheme 2.8. Cyclotetramerization of **2.7** into **2.8**.

In order to isolate the protonated form of the ligand, acid treatment is again used. The solid green powder of the lithiated species is stirred in isopropyl alcohol with acetic acid overnight leading to the clean conversion of the lithiated form to the protonated form. It is then neutralized with potassium hydroxide and all solvent is removed. The remaining solid is dissolved in a mixture DCM and water. An extraction is performed to obtain the DCM layer which is dried under vacuum to obtain a green powder which is the protonated form of the isopropoxy ligand (**Scheme 2.9**).

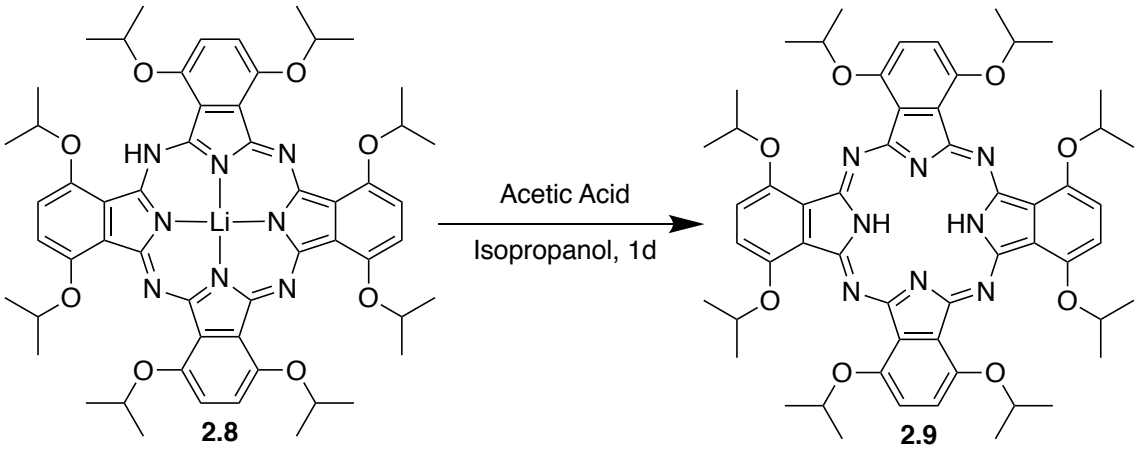

Scheme 2.9. Acidification/demetallation of **2.8** to form **2.9**

The ^{1}H NMR spectrum of **2.9** displays three resonances representative of the various proton environments in the phthalocyanine. There exists a singlet at 7.53 ppm for the aryl protons, as well as a septet and a doublet centered at 4.98 ppm and 1.565 ppm, respectively, for the isopropoxy groups. The N–H resonances could not be located.

Crystals of the following are grown from chloroform and diethyl ether to yield the below structure as green plates. As previously discussed, phthalocyanines tend to twist to form a saddle shape when given bulk substituents (**Figure 2.9**). The isopropyoxy groups cause the phthalocyanine ring to twist to a saddle shape, similar to **2.3**.The bond lengths are very similar in these two structures where the C-$N_{pyrrole}$ bonds have a larger bond

length and the C-N_{linker} bonds are shorter. In **2.3** the range of C-$N_{pyrrole}$ is seen as 1.360(6)-1.385(6) Å, compared with the 1.363-1.403(14) Å lengths seen in **2.9**. When comparing the linker bonds, C-N_{linker} is 1.311(7)-1.352(6) Å in **2.3** whereas the bond lengths in **2.9** are 1.316(17)-1.337(15) Å. These differences in bond length are not too different, and can be reasonably attributed to differences in the twist they have based on the substitutions made.

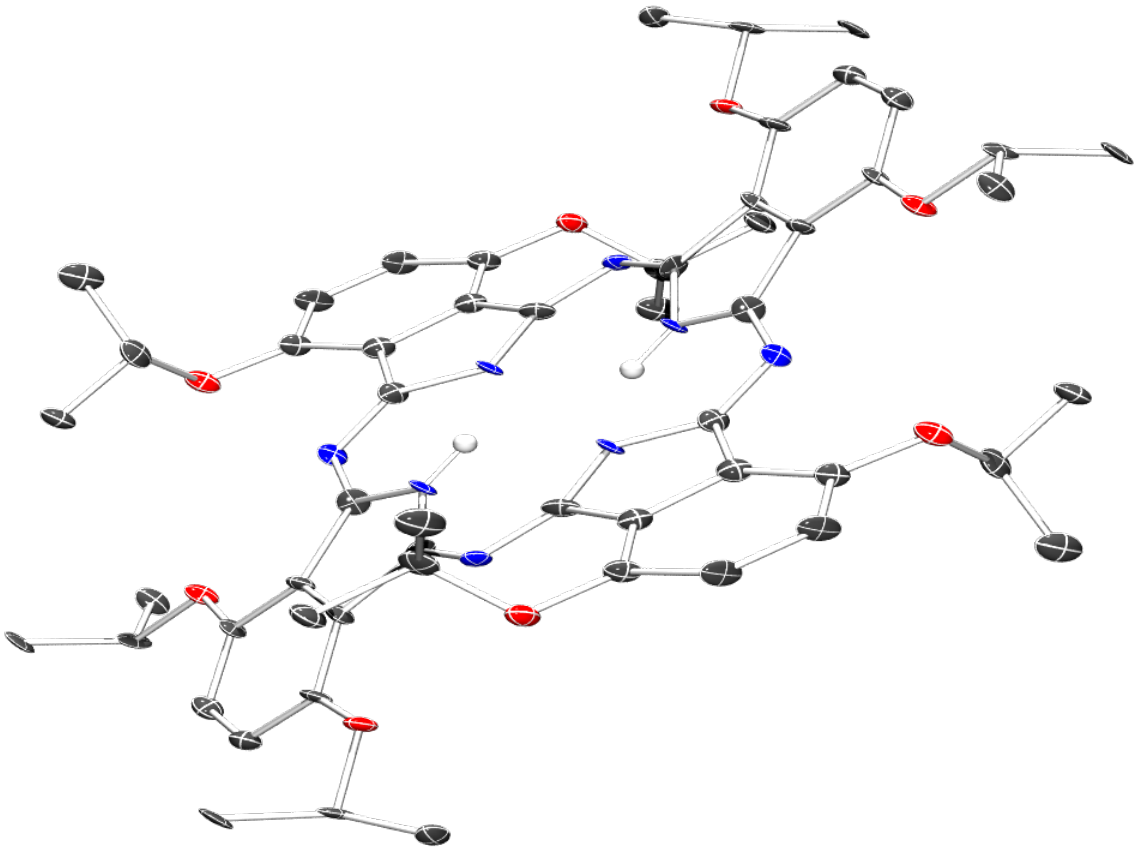

Figure 2.9. Crystal Structure of **2.9**. Protons excluded for clarity, except N-H. Selected bond lengths (Å): N-H: 0.880Å, C-$N_{pyrrole}$: 1.363(14)-1.403(14), C-N_{linker}:1.316(17)-1.337(15).

2.3 Summary

This Chapter described the synthesis of a class of alkoxy-substituted phthalocyanines. Both chromium and manganese complexes of the ethoxy-substituted Pc were generated. The most unique of these is the synthesis of the chromium(II) phthalocyanine as it is the first report of a phthalocyanine being synthesized by the use of a bis(trimethylsilyl)amine salt prior to this. The manganese(II) is able to be oxidized in the presence of air to afford the manganese(III) complex. The removal of its chloride using a silylium salt allows us to have a "naked" manganese center. These complexes are a step towards synthesizing a terminal metal-oxo using the phthalocyanine class of ligands.

The synthesis of the isopropoxy phthalocyanine shows that we can use larger functional groups. This may aid in the trapping a terminal oxo species. Metallation of this complex has been previously accomplished using other first row metals such as nickel, but nothing exists of any other first row metals.

2.4 Experimental

2.4.1 General

All reactions and the following manipulations were carried out under anaerobic and anhydrous conditions with a nitrogen atmosphere by Schlenk or glovebox techniques (MBraun UNIlab Pro SP Eco equipped with a -40 ^{o}C freezer). Pentanes, diethyl ether, dichloromethane, and tetrahydrofuran (Aldrich) were dried using an MBraun Solvent Purification System and stored over 4 Å molecular sieves for 24 hours prior to use. Acetonitrile (Aldrich) was distilled from calcium hydride and stored over 4 Å molecular sieves. Deuterated solvents (Cambridge Isotope Laboratories) were degassed and stored

over 4 Å molecular sieves for 24 hours prior to use. Celite was dried by heating to >250 ^{o}C under dynamic vacuum for at least 24 hours prior to use. $Cr(N(SiMe_3)_2$*2THF was synthesized by a previously published procedure.[29]

NMR spectra were obtained using an Agilent Technologies 400 MHz spectrometer or a Varian Unity Inova 500 MHz spectrometer. Samples were referenced using the residual protio solvent peaks. UV-Vis spectroscopy was performed using a Shimadzu UV-2401PC spectrometer in a quartz cuvette containing a J. Young airtight adaptor.

Mass spectrometry was run at UCSB Chemistry's Mass Spectrometry Facility and all MALDI-TOF was run using a Microflex LRF MALDI TOF spectrometer with a 60 Hz nitrogen laser at 337nm. All ESI data was run on a Waters LCT Premier operated in positive mode by direct injection of the sample in either THF, acetonitrile, or methanol into the instrument.

2.4.2 Synthesis of 3, 6-diethoxyphthalonitrile (2.1)

An adapted literature procedure was used to synthesize the 3, 6-diethoxyphthalonitrile. A 500 mL 2-armed Schlenk flask was charged with 10 g (0.06245 mol) of 2,3-dicyanohydroquinone and 17.26 g (0.1249 mol) of potassium carbonate. A slurry was created by adding 250 mL of acetone. The slurry was brought to reflux and sparged with nitrogen gas for one hour. Following the sparging, 12.5 mL (0.1555 mol) of ethyl iodide was added to the slurry and refluxed under nitrogen gas for 72 hours. It was then pulled from heat and the solution was left to cool. Once cool it was filtered with a medium porosity frit. The solid product was washed with 100 mL of DI

water, then washed with 100 mL of ether. Yield: 8.576 g (0.03965 mol, 63%). ^{1}H ($CDCl_3$): δ 7.14(s, 8H, C_6H_2), 4.13(q,16H, OCH_2), 1.47(t, 24H, CH_3).

2.4.3 Synthesis of Lithiated 1,4,8,11,15,18, 22,25Octaethoxy-29H, 31H-phthalocyanine (LiOEPC) (2.2)

A 500mL 2-armed Schlenk flask was charged with 8.576g (0.03965 mol) of **2.1**. A slurry was created by adding 100 mL of ethanol. The slurry was brought to reflux and sparged with nitrogen gas for one hour. Following the sparging, 10.351g (1.491 mol) of lithium pellets were added to the slurry over a 30 minute period. The resulting solution was refluxed under nitrogen gas for five days. It was then pulled from heat and left to cool**.** Once cooled, 100 mL of ethanol was added to the solution and it was filtered with a fine porosity frit. The solid product was washed with 100 mL of ethanol, then washed with 100mL of DI water, and then washed with 100 mL of ether. Yield: 7.815g (90%, 8.953 mmol) ^{1}H ($CDCl_3$): δ 7.47(m, 8H, C_6H_2), 4.93(m, 16H, -OCH_2), 1.83(m, 24H, CH_3), 14.73(s, 1H, NH). ^{7}Li NMR ($CDCl_3$): δ -8.47 MALDI: $[M]^+$ 872.5m/z, $[M\text{-}Li]^+$ 866.5m/z.

2.4.4 Synthesis of Protonated 1,4,8,11,15,18, 22,25Octaethoxy-29H, 31H-phthalocyanine (H_2OEPC) (2.3)

A 250 mL Schlenk flask was charged with 2.500 g (2.864 mmol) of the **2.2**. A slurry was created by adding 25 mL of ethanol and 25 mL of water. 2.4 mL (0.02904 mol) of concentrated HCl was added slowly to the slurry over a period of 15 minutes. The solution was heated at 45^{o}C for 48 hours. It was then pulled from heat and the solution was allowed to cool. Potassium carbonate was added to the cooled solution in small portions until the pH was ≥7. Once the pH of the solution was ≥7, it was filtered

with a fine porosity frit. The solid product was washed with 25 mL of DI water followed by 25 mL of ethanol and then 25 mL of ether. Yield 2.105 g (81.3%, 2.480 mmol) ^{1}H NMR ($CDCl_3$): δ 7.60 (s, 8H, C_6H_2), 4.95(q, 16H, OCH_2), 1.84(t, 24H, CH_3), 0.20 ppm(s, 2H, NH). MALDI: $[M]^+$ 866.5m/z.

2.4.5 Synthesis of Chromium(II) 1,4,8,11,15,18, 22,25Octaethoxy-29H, 31H-phthalocyanine (CrOEPC) (2.4)

A 50 mL pressure vessel was charged with 500 mg of **2.3** (0.5767 mmol) and 298 mg of $Cr(N(SiMe_3)_2)_2$*2THF (0.5764 mmol). A solution was created by adding 25 mL of THF. The pressure vessel was sealed and then heated to 80^{o}C. The solution was heated for 2.5 hours. It was then pulled from heat and allowed to cool. Once cooled the solution was filtered with a fine fritted funnel. The solid byproduct was washed with 10 mL of THF. The mother liquor was retrieved and dried under vacuum. The crude solid product was stirred with hexanes for 10 minutes. After 10 minutes the solution was filtered with a fine frit. The solid was washed with 10 mL of DI water followed by 10 mL of ethanol. Yield: 0.4569 g (86% yield, 0.4983 mmol) ^{1}H ($CDCl_3$): δ 3.94 (s), 1.86(s). MALDI: $[M]^+$ 916.460m/z. ESI (THF): 1060.4m/z $[M+2THF]^+$. UV-vis λ [nm]: 742, 669, 389, 334.

2.4.6 Synthesis of Manganese(III) Chloride 1,4,8,11,15,18, 22,25Octaethoxy-29H, 31H-phthalocyanine (2.5)

A 100 mL Schlenk flask was charged with 190 mg (0.2192 mmol) of **2.3**, 144 mg (1.144 mmol) of manganese(II) chloride, and 96 mg (1.143 mmol) of sodium bicarbonate. A solution was created by adding 25 mL of DMF. The solution was brought to reflux and refluxed for 5 hours. It was then pulled from heat and left to cool. The solution was then transferred to a 500 mL Erlenmeyer flask. 250 mL of DI water was

added to the solution. The solution was left to cool overnight in a fridge. Once cooled, it was filtered with a fine porosity frit. The solid product was then washed with 30 mL of DI water, then 30 mL of ethanol, and then 30 mL of ether. Yield: 0.160 g (77%, 0.1675 mmol) ^{1}H NMR (CD_2Cl_2): δ 6.72 (s), 1.83 (s), -5.79 (s). MALDI: 954.805 m/z $[M]^+$. UV-vis λ [nm]:826, 747, 562, 349, 277.

2.4.7 Synthesis of "Naked" Mn(III) 1,4,8,11,15,18, 22,25Octaethoxy-29H, 31H-phthalocyanine (2.6)

A 20 mL vial was charged with 10 mg (0.01259 mmol) of triethylsilylium tris(pentafluorophenyl)borane $B(C_6F_5)_4$. A solution was created by adding 2 mL of benzene. A solution of 10 mg of **2.5** (0.01047 mmol) in benzene was added to the vial dropwise and the solution was allowed to stir for two hour. The solution was filtered using a pipette plugged with steel wool and celite. The solid product was then washed with 10 mL of hexanes and then 10 mL of benzene. The solid product was washed off and collected using 5 mL of acetonitrile. The solution was dried under product affording the product. Yield: 0.0159 (95%, 0.009944 mmol) ^{1}H NMR (CD_3CN): Silent. ^{11}B NMR (CD_3CN): δ -16.63(s). ^{19}F NMR (CD_3CN): δ -168.34 (s, 8F, o-C_6F_5), -133.66 (s, 8F, m-C_6F_5), -163.97 (s, 4F, p-C_6F_5). ESI (CH_3CN): 919m/z $[M]^+$, 960.3m/z $[M+CH_3CN]^+$. UV-vis λ [nm]:852, 587, 358, 287.

2.4.8 Synthesis of 3,6-Diisopropoxyphthalonitrile (2.7)

A 250 mL 2-armed Schlenk flask was charged with 1.000 g (6.245 mmol) of 2,3-dicyanohydroquinone and 2.589 g (18.733 mmol) of potassium carbonate. A slurry was created by adding 25 mL of acetone. The slurry was brought to reflux and sparged with nitrogen gas for one hour. Following the sparging, 3.12 mL (31.257 mmol) of 2-

iodopropane was added to the slurry and refluxed under nitrogen for 72 hours. It was then pulled from heat and the solution was left to cool. Once cool it was filtered with a medium porosity frit. The solid byproduct was washed with 50 mL of acetone. The mother liquor was retrieved and dried under vacuum to half the volume. 150 mL of DI was added to the solution. The solution was then filtered with a fine porosity frit. The solid product was washed with 25 mL of water. Yield: 0.781 g (51%, 3.187mmol) ^{1}H ($CDCl_3$): δ 7.15(s, 2H, C_6H_2), 4.57(sep, 2H, OCH), 1.39(d, 12H, CH_3).

2.4.9 Synthesis of Lithium 1,4,8,11,15,18,22,25-Octaisopropyl-29H,31 H-Phthalocyanine (2.8)

A 500 mL 2-armed Schlenk flask was charged with 2.30 g (9.415 mmol) of **2.7**. A slurry was created by adding 75 mL of isopropyl alcohol. The slurry was brought to reflux and sparged with nitrogen gas for one hour. Following the sparging, 2.00 g (288.1 mmol) of lithium pellets were added to the slurry over a 45 minute period. The resulting solution was refluxed under nitrogen gas for 72 hours. It was then pulled from heat and left to cool**.** Once cooled the solution was filtered with a fine porosity frit. The solid product was washed with 20 mL of isopropyl alcohol, and then washed with 100 mL of DI water. Yield: 0.820 g (35%, 0.8324 mmol)

2.4.10 Synthesis of 1,4,8,11,15,18,22,25-Octaisopropyl-29H,31 H-Phthalocyanine (2.9)

A 20 mL vial was charged with 100 mg (0.1015 mmol) of **2.8**. A slurry was created by adding 3.8 mL of isopropanol. 0.6 mL (10.481 mmol) of acetic acid was added to the slurry and it was left to stir overnight. The following day, 5 mL of water was added to the slurry and then the solution was neutralized with potassium hydroxide pellets.

Once the solution had a pH of approximately 7, the solution was dried under vacuum. The solid product was stirred with DCM and water for 30 minutes. After 30 minutes the DCM layer was extracted from the mixture. The DCM was dried under vacuum to yield the solid product. Yield: 0.0796 g (80%, 0.08129 mmol) ^{1}H NMR ($CDCl_3$): δ 7.53 (s, 8H, C_6H_2), 4.98 (sep., 8H, OCH), 1.57 (d, 48H, CH_3).

2.5 References

1. Bekaroglu, O., History, development, and a new concept of phthalocyanines in Turkey. *Turk. J. Chem.* **2014,** *38* (6), 903-922.

2. J., B. P.; J., G. S.; A., O. O.; Lester, W., Improved synthesis of metal-free phthalocyanines. *J. Heterocycl. Chem.* **1970,** *7* (6), 1403-1405.

3. Leznoff, C. C.; Lever, A. B. P., *Phthalocyanines: Properties and Applications* VCH Publishers: New York, 1989.

4. Sakamoto, K.; Ohno-Okumura, E., Syntheses and Functional Properties of Phthalocyanines. *Materials* **2009,** *2* (3), 1127-1179.

5. Uchida, H.; Mitsui, M.; Reddy, P. Y.; Nakamura, S.; Toru, T., Convenient synthesis of phthalocyanines with disilazanes under mild conditions. *Arkivoc* **2005**, 17-23.

6. Drager, A. S.; O'Brien, D. F., Novel synthesis of liquid crystalline phthalocyanines. *J. Org. Chem.* **2000,** *65* (7), 2257-2260.

7. Sorokin, A. B., Phthalocyanine Metal Complexes in Catalysis. *Chem. Rev.* **2013,** *113* (10), 8152-8191.

8. Contakes, S. M.; Beatty, S. T.; Dailey, K. K.; Rauchfuss, T. B.; Fenske, D., pi-complexes of phthalocyanines and metallophthalocyanines. *Organometallics* **2000,** *19* (23), 4767-4774.

9. Zhou, W.; Thompson, J. R.; Leznoff, C. C.; Leznoff, D. B., The Redox-Active Chromium Phthalocyanine System: Isolation of Five Oxidation States from (Pc4-CrI) to (Pc2-CrIII). *Chen, Eur. J.* **2017,** *23* (10), 2323-2331.

10. Sanchez, M.; Fache, E.; Bonner, D.; Meunier, B., Synthesis of organo-soluble metallophthalocyanines bearing electron-withdrawing substituents. *J.Porphyrins Phthalocyanines* **2001**, 867.

11. Barrett, P. A.; Dent, C. E.; Linstead, R. P., Phthalocyanines. Part V I I . Phthalocyanine as a Co-ordinating Group. A General Investigation of the Metallic Derivatives. *J. Chem. Soc.* **1936**, 1719.

12. Elvidge, J. A.; Lever, A. B. P., Metal Chelates .2. Phthalocyanine-Chromium Complexes and Perpendicular Conjugation. *J. Chem. Soc.* **1961,** (Mar), 1257-&.

13. Georgescu, R.; Boscornea, C.; Calinescu, I.; State, R., Raman, IR and UV-Vis Spectroscopic Investigations of Some Substituted Phthalocyanines. *Rev. Chim. Bucharest* **2015,** *66* (10), 1554-1557.

14. Ghani, F.; Kristen, J.; Riegler, H., Solubility Properties of Unsubstituted Metal Phthalocyanines in Different Types of Solvents. *J. Chem. Eng. Data* **2012,** *57* (2), 439-449.

15. Chernonosov, A. A.; Ermilov, E. A.; Roder, B.; Solovyova, L. I.; Fedorova, O. S., Effect of Some Substituents Increasing the Solubility of Zn(II) and Al(III) Phthalocyanines on Their Photophysical Properties. *Bioinorg. Chem. Appl.* **2014**.

16. Chen, Y. X.; Fang, W. J.; Wang, K.; Liu, W.; Jiang, J. Z., Nonperipheral Tetrakis(dibutylamino)phthalocyanines. New Types of 1,8,15,22-Tetrakis(substituted)phthalocyanine Isomers. *Inorg. Chem.* **2016,** *55* (18), 9289-9296.

17. Isabirye, D. A.; Seheri, N. H.; Aiyelabola, T. O., Synthesis and Structural Characterization of Cr(III) Complex of Pophyrazine and Phthalocyanine Derivatives: Kinetics Studies of Metalation and Redox Activity *Asian J. Chem.* **2017,** *29* (3), 489-495.

18. Hunt, C. C.; Peterson, M.; Anderson, C.; Wu, G.; Scheiner, S.; Sepunaru, L.; Ménard, G., Manuscript in preparation

19. Liao, M. S.; Scheiner, S., Electronic structure and bonding in metal phthalocyanines, Metal=Fe, Co, Ni, Cu, Zn, Mg. *J. Chem. Phys.* **2001,** *114* (22), 9780-9791.

20. Liao, M. S.; Scheiner, S., Electronic structure and bonding in metal porphyrins, metal=Fe, Co, Ni, Cu, Zn. *J. Chem. Phys.* **2002,** *117* (1), 205-219.

21. Eikey, R. A.; Abu-Omar, M. M., Nitrido and imido transition metal complexes of Groups 6-8. *Coord. Chem. Rev.* **2003,** *243* (1-2), 83-124.

22. Janson, T. R.; Kane, A. R.; Sullivan, J. F.; Knox, K.; Kenney, M. E., Ring-Current Effect of Phthalocyanine Ring. *J. Am. Chem. Soc.* **1969,** *91* (19), 5210-&.

23. Iwamoto, H.; Hori, K.; Fukazawa, Y., A model of porphyrin ring current effect. *Tetrahedron Lett.* **2005,** *46* (5), 731-734.

24. Abraham, R. J.; Medforth, C. J., The Nmr-Spectra of the Porphyrins .36. Ring Currents in Octaethylporphyrin, Meso-Tetraphenylporphyrin and Phthalocyanine Complexes. *Magn. Reson. Chem.* **1988,** *26* (9), 803-812.

25. Yamada, K.; Suwa, Y.; Katagiri, C.; Nakayama, K., High vertical carrier mobility in the nanofiber films of a phthalocyanine derivative and its application to vertical-type transistors. *Org. Electron.* **2018,** *53*, 320-324.

26. Engel, M. K.; Hokoku, K. R. K., *Single-Crystal and Solid-State Molecular Structures of Phthalocyanine Complexes*. Academic Press: Amsterdam, 1997; Vol. 20.

27. Sun, X.; Wang, L.; Tan, Z., Improved Synthesis of Soluble Metal-Free/Metal Phthalocyanine Tetracarboxylic Acids and Their Application in the Catalytic Epoxidation of Cyclohexene. *Catal. Lett.* **2015,** *145* (4), 1094-1102.

28. Jiang, Y. F.; Chakarawet, K.; Kohout, A. L.; Nava, M.; Marino, N.; Cummins, C. C., Dihydrogen Tetrametaphosphate, P4O12H2 (2-): Synthesis, Solubilization in Organic Media, Preparation of its Anhydride P4O11 (2-) and Acidic Methyl Ester, and Conversion to Tetrametaphosphate Metal Complexes via Protonolysis. *J. Am. Chem. Soc.* **2014,** *136* (34), 11894-11897.

29. Deng, Y. F.; Han, T.; Wang, Z. X.; Ouyang, Z. W.; Yin, B.; Zheng, Z. P.; Krzystek, J.; Zheng, Y. Z., Uniaxial magnetic anisotropy of square-planar chromium(II) complexes revealed by magnetic and HF-EPR studies. *Chem. Commun.* **2015,** *51* (100), 17688-17691.

30. Wang, H. H.; Yuan, H. Q.; Mahmood, M. H. R.; Jiang, Y. Y.; Cheng, F.; Shi, L.; Liu, H. Y., Crystal structure, magnetic and catalytic oxidation properties of manganese(III) tetrakis(ethoxycarbonyl)porphyrin. *RSC Adv.* **2015,** *5* (118), 97391-97399.

31. Lambert, J. B.; Zhang, S. Z.; Ciro, S. M., Silyl Cations in the Solid and in Solution. *Organometallics* **1994,** *13* (6), 2430-2443.

32. Cortes, S. A.; Hernandez, M. A. M.; Nakai, H.; Castro-Rodriguez, I.; Meyer, K.; Fout, A. R.; Miller, D. L.; Huffman, J. C.; Mindiola, D. J., Titanium complexes supported by a sterically encumbering N-anchored tris-arylphenoxide ligand. *Inorg. Chem. Commun.* **2005,** *8* (10), 903-907.

33. Yu, L.; Zhou, X.; Yin, Y.; Li, R.; Peng, T., 4,5-Bis(4-meth-oxy-phen-oxy)phthalonitrile. *Acta Crystallogr. Sect. E: Struct. Rep. Online* **2010,** *66* (Pt 10), o2527-o2527.

Chapter 3: Synthesis and Characterization of Metal Oxo Species

3.1 Introduction

As previously discussed, metal-oxos have been prepared from systems similar to the phthalocyanine species synthesized in Chapter 2. In general there is an electronic criterion for the syntheses of metal-oxos. An electron count of d^2 is favored in order to stabilize a metal oxygen triple bond with a C_{4v} square pyramidal geometry.[1] This is due to repulsion between the higher d electron count and the oxo ligand itself, which causes the oxygen not to form multiple bonds with the metal species.[2] The "oxo wall" is the theory that describes this and it refers to the inability of complexes with d-electron counts larger then five to form terminal oxo complexes.[3-4] **Figure 3.1** shows the d-orbital splitting in square pyramidal structures, as the electron count goes past four d-electrons, antibonding orbitals become populated causing the inability to form a terminal oxo.

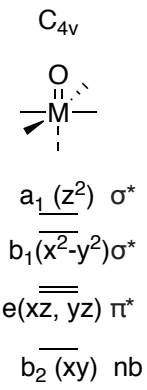

Figure 3.1. Molecular orbital diagram for a basic square pyramidal structure with ligand orbitals excluded.

Several approaches have been taken when it comes to forming metal oxo species. One method uses high valent metal species as the starting materials for formation of the oxo, and another method makes use of a ligand in which the oxo can be trapped or stabilized to form the stable metal oxo. The work of the Goldberg group to synthesize the corrolazine ligands, which can bind a metal with a charge of 3+, uses the first approach.[5-

[15] Having a high valent metal starting material removes electrons from the d orbitals. This is useful as there is less electron density to repel against the binding of the oxo ligand. With a manganese(III), simple addition of an O-atom donor affords the corresponding metal oxo product. Aside from its ability to react with an O-atom donor to get the oxo, this species reacts with molecular oxygen in the presence of UV-light to form a manganese-oxo species.[7, 10-12, 16-18]

The second approach used ligand modifications that aid in trapping or stabilizing of the metal-oxo bond. The "picket fence" porphyrin is the prime example of a trapping ligand. Using large, bulky substitutions on the bridging carbons of the porphyrin ring, the metal helps to attract the oxygen and the bulky substituents help to "trap" the bound oxygen (**Fig 3.2**). This ligand and its iron species has been used extensively in order to model heme proteins such as myoglobin and hemoglobin.[19-24]

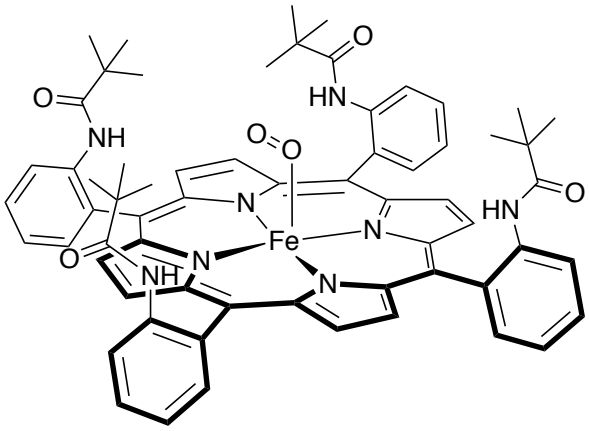

Figure 3.2. "Picket fence" porphyrin with trapped oxygen bound to the metal center.

Another such form of trapping an oxo is seen in the hangman corrole. The hangman corrole has a side chain extending from the central pyrrole ring linker that aids in the bonding of an oxygen atom to the central metal of the corrole. The cobalt(III) corrole synthesized by the Nocera group is capable of binding water to the central metal

and it is able to oxidize the water molecule to electrocatalytically form dioxygen. The side chain is used to stabilize the oxo with its ability to hydrogen bond with the oxo species. The side chain is also capable of attracting a second molecule of water with hydrogen bonds to react with the oxo. **Figure 3.3** shows water reacting with a cobalt oxo which will lead to the formation of dioxygen.[25-28]

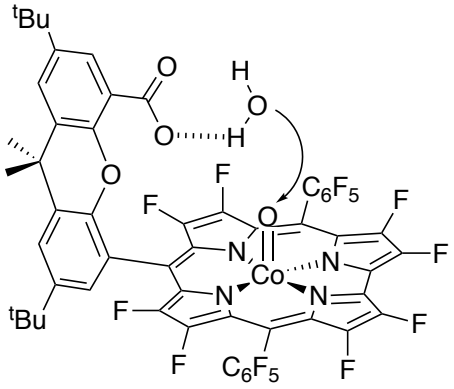

Figure 3.3. Hangman corrole attracts water and uses hydrogen bonding to electrochemically form O_2.

In this chapter, the synthesis of vanadyl phthalocyanine species with both ethoxy and isopropoxy phthalocyanine ligands will be explored. Descriptions of different attempts to synthesize and characterize chromium and manganese oxo are also included. In addition, potential future experimentation will be discussed using preliminary data from this work.

3.2 Results and Discussion

3.2.1 Vanadyl(IV) Octaethoxyphthalocyanine Synthesis and Characterization (3.1)

The synthesis of the vanadyl phthalocyanine species is modified from a reported synthesis by Rauchfuss.[29] The vanadyl phthalocyanine is similarly made to the other metal phthalocyanines, from the protonated (**2.3**) or lithiated (**2.2**) form of the ligand. An excess of vanadyl sulfate and sodium biocarbonate is added to a solution of refluxing

solution of protonated (**2.3**) or lithiated (**2.2**) phthalocyanine in DMF. This solution is refluxed for 5 hours, after which time it is cooled and water is added to precipitate out the metallated phthalocyanine product. Filtration of the product yields a dark green powder at 69% yield. Crystals for this species can be grown from DCM and ether (**Scheme 3.1**).

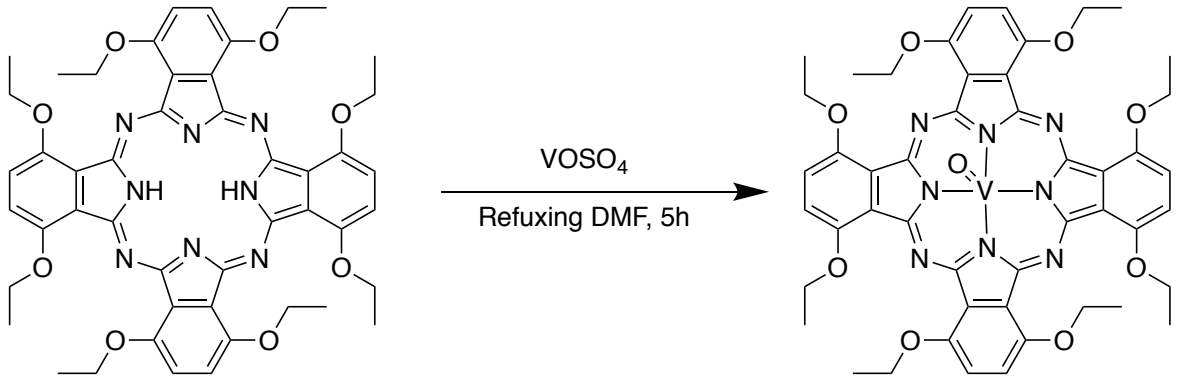

2.3 **3.1**

Scheme 3.1. Synthesis of **3.1**

The ^{1}H NMR spectrum of the product in $CDCl_3$ reveals three broadened signals, despite having a paramagnetic metal center. The three signals are located at 8.50 ppm, 5.03 ppm and 1.88 ppm. These signals integrate to 8, 16, and 24 respectively. It is likely that the 8.50 ppm signal references the aryl protons in the phthalocyanine and the two signals at 5.03 ppm and 1.88 ppm refer to the ethoxy groups. Attempts were made to do ^{51}V NMR on the species, but as it is a paramagnetic species, the signal is too broad to observe.

Low Temperature EPR spectroscopy was run on **3.1** to confirm the presence of vanadium and to compare it to other vanadyl C_{4v} species. The spectrum was taken in DMF and yielded the spectrum seen in **Figure 3.4**. The $g_{||}$ value was found to be approximately 2.10 and $g_{\perp}$ was found to be approximately 2.00. The hyperfine coupling

constant were found to be 44 MHz and 169 MHz for $a_{||}$ and $a_{\perp,}$ respectively.[29] These values are almost identical to those reported by Rauchfuss, where the $g_{||}$ value was 2.139 and $g_{\perp}$ was approximately 2.0048. In addition, the hyperfine coupling constant were 45 MHz and 168 MHz for $a_{||}$ and $a_{\perp,}$ respectively.[29]

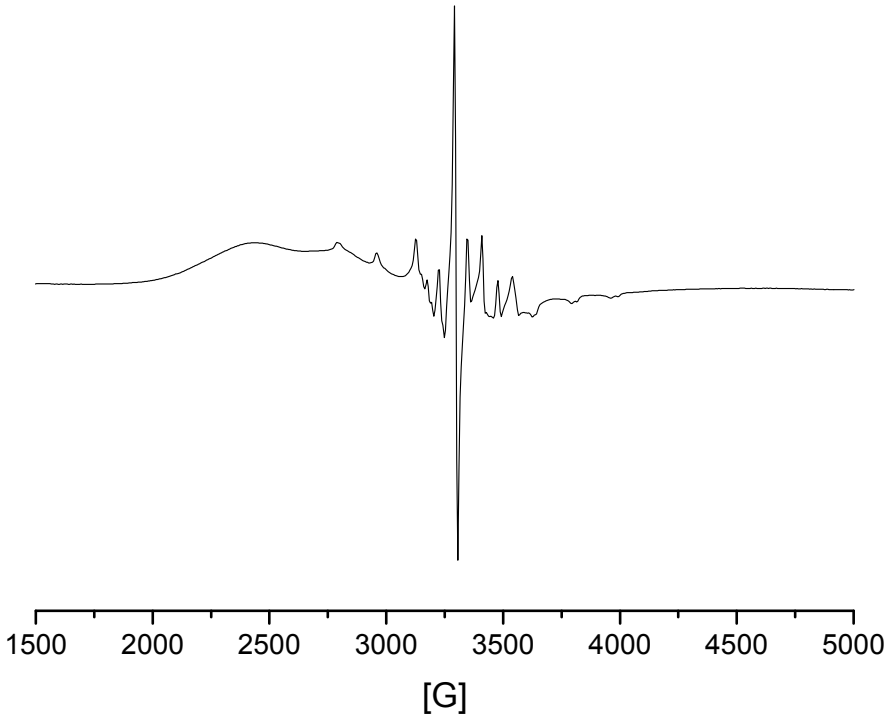

Figure 3.4. EPR spectrum of V=O(IV)OEPC taken at 100 K in frozen DMF.

ESI was run on **3.1** in THF and this yielded a molecular ion peak at 931.4 m/z. A [M+1] peak was located at 932.4 m/z. These peaks overlap making the isotopic splitting unclear.

Crystals of **3.1** are grown as green hexagonal plates from a solvent system of chloroform and ether. The refined structure is seen in **Figure 3.5.**The most significant bond in this structure is that of the V=O. The structure is interesting as it contains a puckering of the vanadium out of the center of the pocket. The phthalocyanine ligand

itself is not planar, but rather it has more of a saddle shape with two groups. The vanadyl bond length is shorter, but comparable to the bond lengths seen in vanadyl porphyrin and phthalocyanine systems. In vanadyl porphyrins and unsubstituted vanadyl phthalocyanines, the vanadyl bond has lengths of 1.620 and 1.580 Å respectively. The bond length seen in **3.1** is shorter having a length of 1.576(6).[30-31]

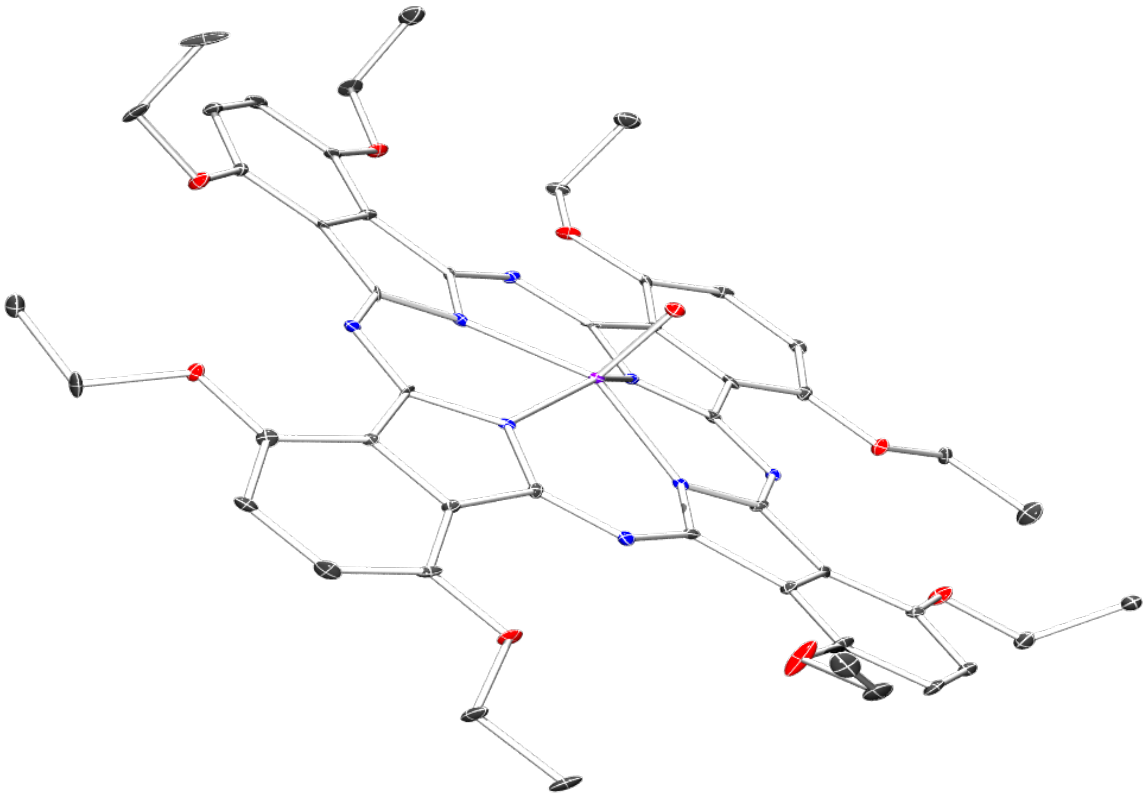

Figure 3.5. The crystal structure of **3.1**. Selected bond lengths: V=O: 1.576(6) Å N1-V: 2.033(8) Å, N2-V: 2.063(7) Å, N3-V: 2.043(7) Å, N4-V: 2.036(7) Å

3.2.2 Vanadyl (IV) Octaisopropoxyphthalocyanine Synthesis and Characterization (3.2)

Metallated octaisopropoxyphthalocyanine (OIPC) has been synthesized previously, but only a nickel phthalocyanine is known.[29] The vanadyl isopropoxyphthalocyanine is easily synthesized by adding excess vanadyl sulfate and

excess sodium bicarbonate to a solution of refluxing protonated **(2.9)** or lithiated phthalocyanine **(2.8)** in DMF. This solution is refluxed for two hours, after which time it is cooled and water is added to precipitate out the vanadyl phthalocyanine product (**Scheme 3.2**). The reaction had a yield of 26%.

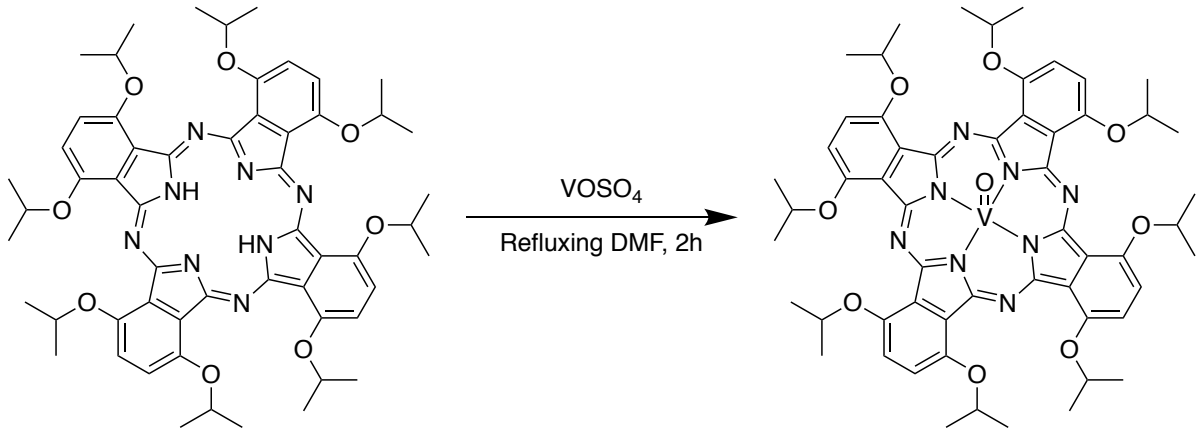

2.9 **3.2**

Scheme 3.2. Synthesis of the vanadyl isopropoxyphthalocyanine (**3.2**)

ESI was run on the species in methanol and it yielded a molecular ion peak at 1043.4 m/z. In addition to the [M]+ peak there was a [M+1] peak that appeared at 1044.5 m/z. These overlapping signals made confirmation of the isotopic splitting difficult, but confirm the existence of the desired species as a product of this reaction.

3.2.3 Attempts at a Chromium Oxo

Chromium oxos are known in corroles and in porphyrins as well. Similar to some of the manganese corrole systems, the use of O-atom donors, such as m-CPBA or iodosobenzene is useful in the formation of the terminal oxo in both the porphyrin and corrole ligand frameworks.[32-33] For our system, we examined whether the use of an O-atom donor would generate a terminal Pc-Cr oxo. Use of iodosobenzene as an O-atom donor was tested first (**Scheme 3.3**). Iodosobenzene on transfer of an O-atom reverts to

become iodobenzene, which can easily be observed by ^{1}H NMR. Accordingly, the reaction of iodosobenzene with the chromium(II) phthalocyanine was run in the d_3-acetonitrile in a sealed J. Young NMR tube. No color change was observed in the reaction solution and further evaluation by NMR proved no conversion to iodobenzene. Furthermore, ESI showed no proof of a bridging or terminal oxo.

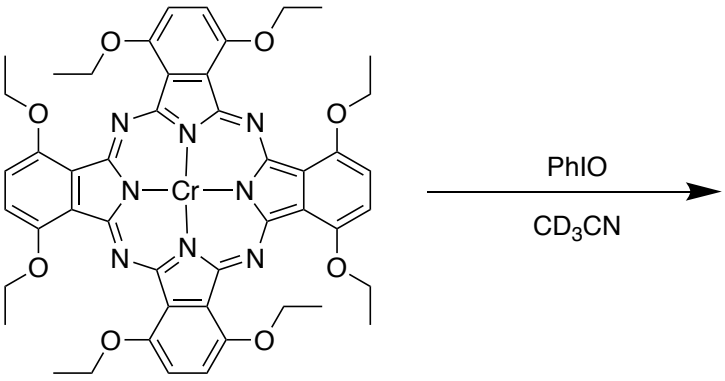

2.4

Scheme 3.3. Reaction of **2.4** with Iodosobenzene in Deuterated Acetonitrile.

Hypochlorite proves to be a very useful oxidant in the synthetic route for synthesis of manganese nitrides of both phthalocyanines and salen complexes.[34-36] Therefore, it is possible that hypochlorite could form an oxo with the phthalocyanine in the presence of air. Chromium(II) phthalocyanine was dissolved in methanol and cooled to -78^{o}C and bleach was added in excess as the reaction stirred. After a half hour, the reaction had changed from green in color to an orange-yellow color. An extraction was performed using DCM and water. The DCM layer containing the orange-yellow product was separated from the water used to separate out unreacted bleach. The DCM was dried and MALDI-TOF was run on the produced species. The spectrum of this species did not

show an oxo species, but rather a hydroxo species. Attempts to recrystallize and confirm that the identity of the species was indeed a hydroxo chromium species have been unsuccessful (**Scheme 3.4**)

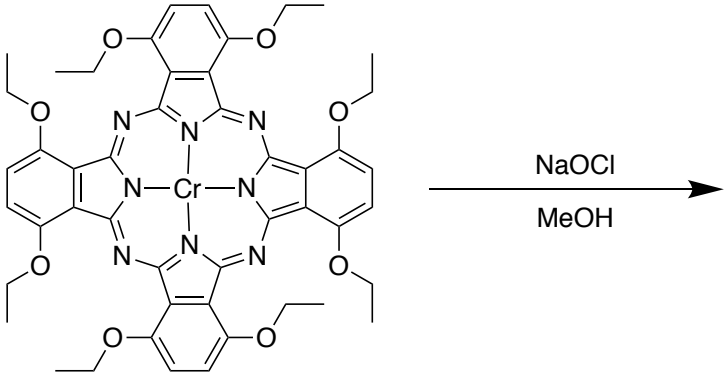

2.4

Scheme 3.4. Reaction of **2.4** with hypochlorite in bleach.

3.2.4 Attempts at a Manganese Oxo

As noted in Chapter 1, there are a few examples of manganese oxo corroles. Using a manganese(III) species and an O-atom donor or oxidant afforded a manganese oxo product. Goldberg was able to use *m*-CPBA, iodosobenzene and air as oxidants to produce a manganese oxo from manganese(III) corroles and corrole derivatives.[7, 16-18] In addition, there are reports of porphyrin manganese-oxos being formed using hypochlorite.[34-35]

When the manganese(III) chloride was dissolved in methanol and cooled to -78^{o}C, addition of excess bleach solution to this stirring solution yields an orange brown solution (**Scheme 3.5**). DCM was stirred into the solution after a half hour, and an extraction of the DCM using water to remove excess bleach was performed. The orange brown DCM solution was dried and afforded an orange brown product. The ^{1}H NMR

spectrum of this species offers a few broadened signals very similar to that of the manganese(III) chloride solution. There is no evidence that the oxidant caused the phthalocyanine ring to decompose to form its precursor or fragmented units. The MALDI data shows no evidence of the starting material, a terminal oxo, or even a bridging oxo species. However, a signal does appear in the MALDI spectrum at 936.679 m/z. This species is very possibly a manganese (III) hydroxide. Attempts to grow crystals of the product from a number of solvent systems have been fruitless, with solutions often forming oily and/or powdery products.

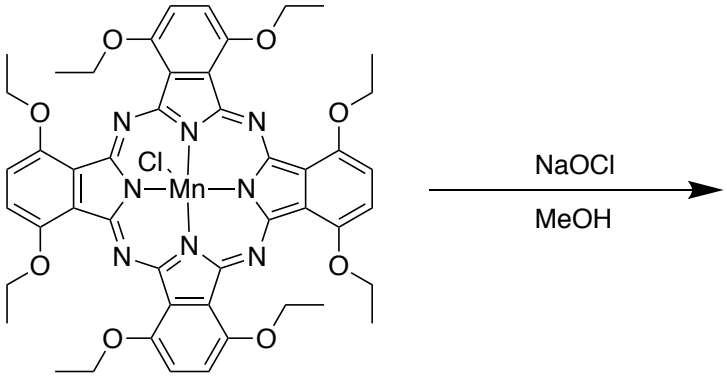

2.5

Scheme 3.5. Reaction of **2.5** with bleach.

Further attempts were made using m-CPBA, as it was seen as a successful reagent by the Goldberg group in their conversion of manganese(III) corrolazines into manganese oxos.[7] A solution was prepared of 1 equivalent of manganese(III) chloride phthalocyanine dissolved in 5 mL of DCM. 1 equivalent of the m-CPBA dissolved in DCM was added to this red solution. The solution was stirred for a few hours after which no color change was noted. The reaction was left to stir overnight after which no change had occurred. A MALDI-TOF analysis confirmed that no reaction had occurred (**Scheme**

3.6). Similar reactions using 1 equivalent of other O-atom donors, such as iodosobenzene yield a similar result of no reaction.

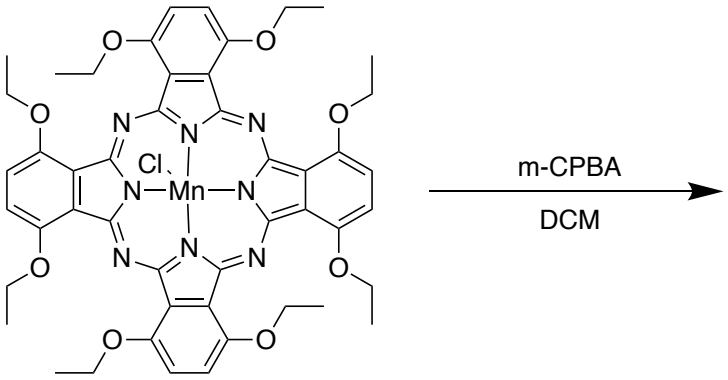

2.5

Scheme 3.6. Reaction of m-CPBA with **2.5**.

At this point, we considered whether the presence of the chloride may be a potential issue in the formation of an oxo species. In all of the corrolazine examples explored there was no axial ligand present prior to formation of the metal oxo. Attempts to synthesize and isolate a "naked" manganese(III) phthalocyanine (**2.6**) became successful through the use of $[Et_3Si][B(C_6F_5)_4]$. This reagent removes the chloride, and replaces it with an outer-sphere anion, $B(C_6F_5)_4^-$, leaving the axial sites on the manganese free for bonding. [37-38] The same reactions that were attempted with the manganese(III) chloride species were repeated with the now "naked" manganese(III) phthalocyanine. The newly synthesized species was first tested with O-atom donors in THF, as its solubility is very limited to coordinating solvents. 1:1 reaction with m-CPBA in THF did not immediately yield a color change or any noticeable reaction (**Scheme 3.7**). When left to stir overnight the solution seems to have polymerized. The "naked" manganese(III) species is soluble in THF, and does not appear to react with it when left to sit in THF,

however, the products of the reaction seemed to have caused polymerization of THF (**Scheme 3.7**).

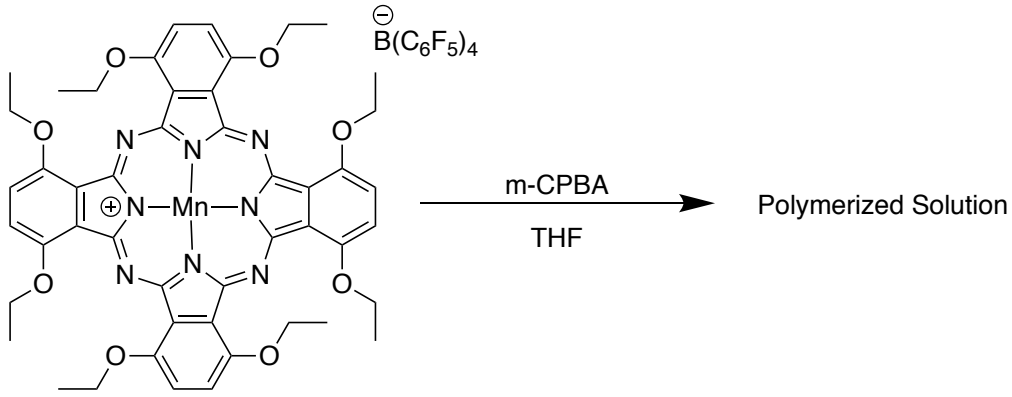

2.6

Scheme 3.7. Reaction of **2.6** with m-CPBA in THF causes polymerization of THF.

Further reactions were tested using acetonitrile, which forms a blue solution with the manganese complex. Acetonitrile does not polymerize as readily as THF, which makes it a more suitable solvent. We next attempted the analogous reaction of **2.6** with *m*-CPBA in acetonitrile (**Scheme 3.8**). The reaction with m-CPBA was fast, as it begins to change color with stirring after ca. 5 min changing colors from blue to a reddish-brown. Attempts were made to characterize this reaction by MS, but the ESI of the spectra only shows the starting naked manganese species. UV-Vis shows the reaction occurring over a short span of time. In **Figure 3.6,** the spectrum of the reaction can

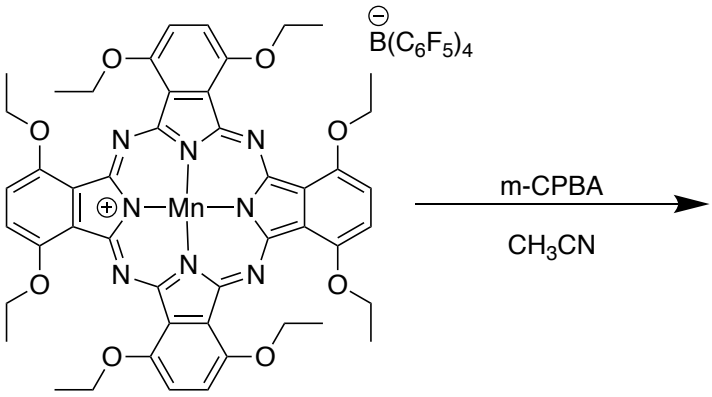

2.6

Scheme 3.8. Reaction of **2.6** with m-CPBA causes the solution to go from a blue to a reddish color.

be seen as it reacts over time. The spectrum shows a blue shift of the Q-Band from 852 nm to 837 nm as the reactants convert to the products. The change happens rapidly with the product completely forming after a little more than an hour. The black trace represents the reaction at its start and the red trace shows the product after the reaction is completed.

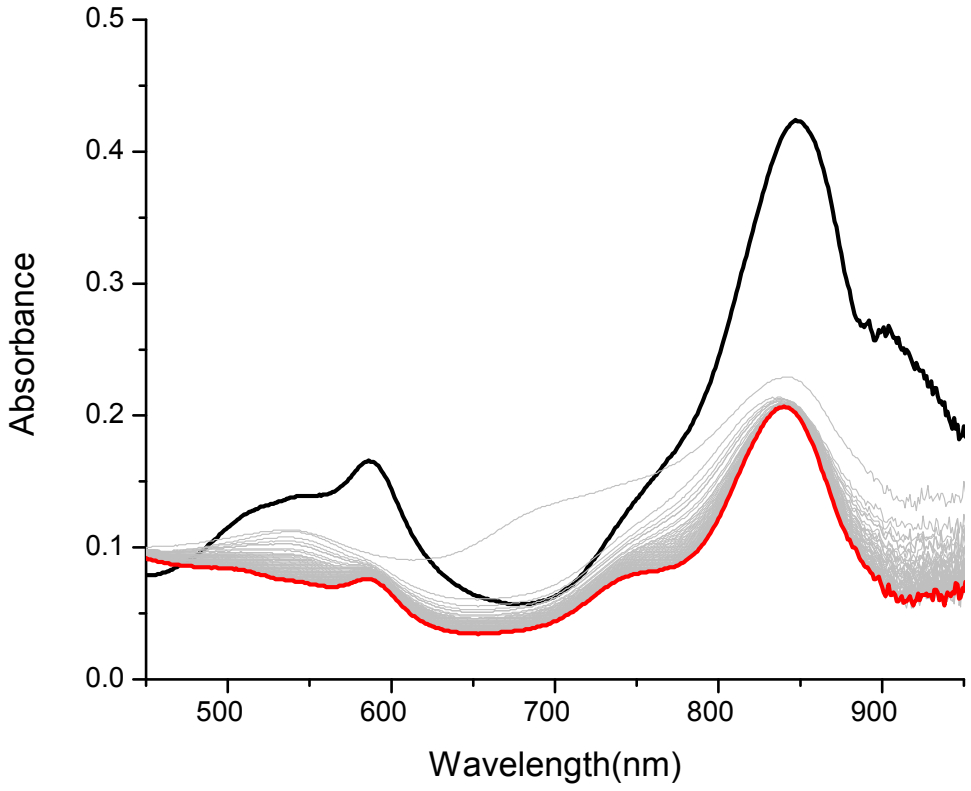

Figure 3.6. UV-Vis spectrum of the "naked" manganese phthalocyanine and its reaction with m-CPBA. Reaction run in acetonitrile, with a 90 second acquisition delay over a 2.5 hour span. The black trace represents the starting material and the red trace represents the product, the grey traces show the transition from starting material to product over time.

Similar attempts were made using iodosobenzene over time in the UV-Vis, but the poor solubility of the iodosobenzene in acetonitrile made the reaction difficult to track over time. However, this species seems to be reactive with molecular oxygen (**Scheme 3.9**) similarly to the Goldberg manganese corrole. An equivalent was dissolved in acetonitrile and placed in a UV-Vis cell. An initial scan was run to mark the starting spectrum, and then a needle was used to introduce oxygen to the airtight UV cell (**Scheme 3.9**). 100 scans were run over a fifteen hour period and show a blue shift to a new product as can be seen in **Figure 3.7**. The black trace with the least absorbance

shows the starting material and over fifteen hours this signal has a blue shift to the product species. Attempts to crystallize this product have been ineffective and the mass spectrum of this species is similarly useless, as it shows signal at the same value as the "naked" manganese.

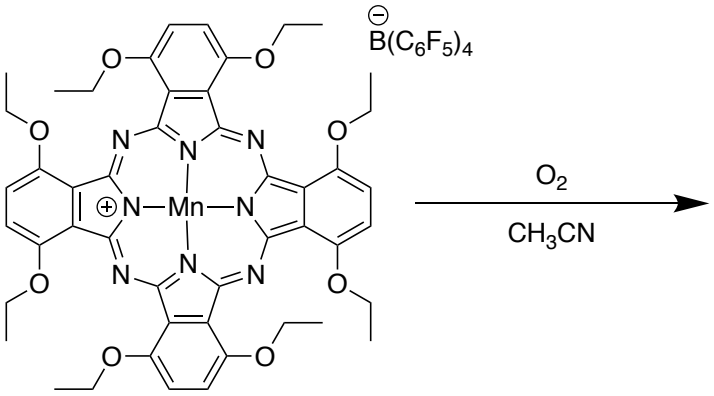

2.6

Scheme 3.9. In solution **2.6** reacts with air going from a blue solution to a reddish colored solution.

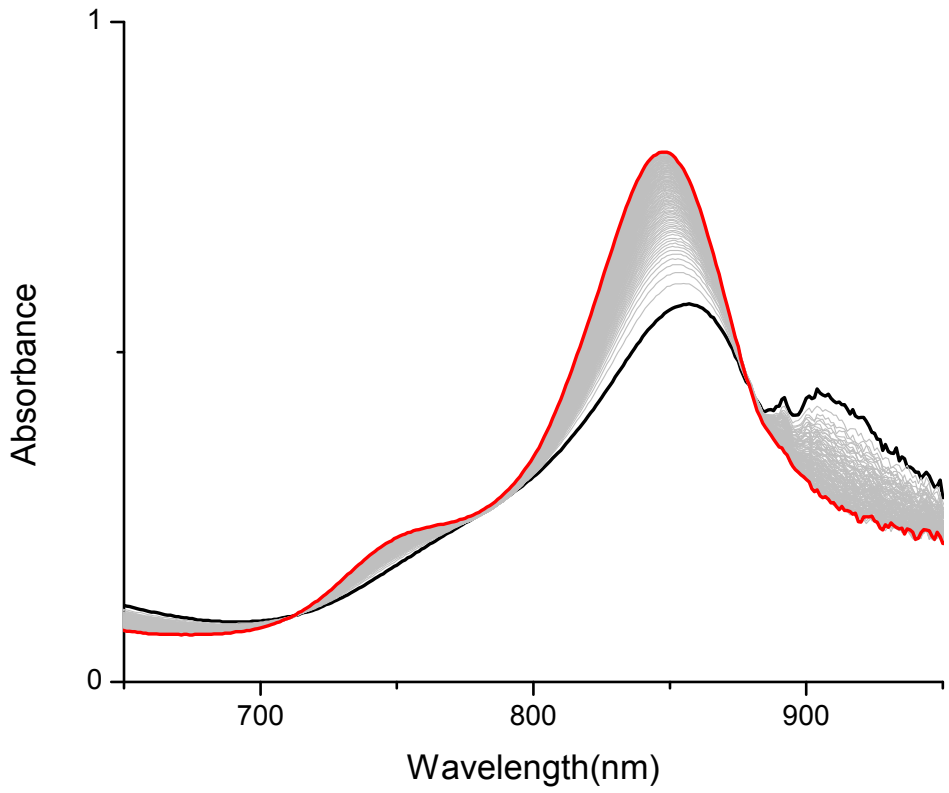

Figure 3.7. UV-Vis spectrum of airs reaction with the "naked" manganese phthalocyanine species. Reaction run in acetonitrile over 15 hours with a 9 minute acquisition delay time. The black trace represents the starting material and the red trace represents the product, the grey traces show the transition from starting material to product over time. The reaction is much slower with O_2 but shows the same shift.

Further study of these two reactions and other reactions of the "naked" manganese species could be useful in isolation of a manganese-oxo phthalocyanine species. The "naked" manganese species is reactive and might prove to be an invaluable starting material for the synthesis of an oxo species.

3.3 Future Work

In this chapter there has been convincing evidence that an oxo can be formed using a naked manganese phthalocyanine. Further evaluation of this species and its reactivity could be useful in developing a strategy to synthesize a manganese oxo bond. As stated in the introduction, it is favorable to have a lower electron count in order to

synthesize an oxo species, as more electrons in the d orbitals will cause repulsion between the metal and the oxo ligand. This could develop into a good strategy to aid in the formation of a chromium species as well. Previous attempts to synthesize a chromium(III) phthalocyanine species have not been as successful as the synthesis of isolated chromium(II) species. However, a chloride donor such as trityl chloride could be used to convert the chromium(II) to a chromium(III) species. This species can be tested for reactivity with O-atom donors first to ensure that it is not a reactive species and a good pathway to a chromium-oxo. If this is unsuccessful, further modification of the chromium species to remove the chloride, creating a "naked" chromium phthalocyanine could be beneficial to the synthesis of an oxo.

If these modifications to the metal center prove fruitless, changes to the ligand framework could prove useful. The ligand synthesized by the Goldberg group starts as a porphyrazine and removal of one of the bridging nitrogen atoms affords them a corrolazine.[5] It is possible that similar reactions of the phthalocyanine can afford a triazatetrabenzcorrole, which is a similar framework. Alternatively, following literature to synthesize this ligand and use it to synthesize a 3- ligand would be beneficial and potentially useful as starting from a 3+ metal has proven to be a more reactive start point for making a metal oxo species with corroles.[39-40]

If a phthalocyanine oxo is synthesized, the potential for the species to be used in C-H bond activation can be explored. Studies can be conducted to confirm or deny the ability of the synthesized oxo to perform this C-H cleavage reaction, as the manganese-oxo's of the Goldberg group are capable of breaking the C-H bonds of phenols.[7-8, 10]

Alternatively, the two potential hydroxo species, synthesized by the addition of hypochlorite to a solution containing either chromium or manganese phthalocyanine could be of potential use. The hydroxide species synthesized by the Goldberg group were also effective C-H bond activation catalysts and if either the chromium or the manganese hydroxo phthalocyanine can be isolated in good yield, they may be capable of C-H activation catalysis.[16]

Lastly, additional species could be synthesized using the isopropoxyphthalocyanine. A study to determine if the ligand does help to trap the phthalocyanine oxo could prove useful. It would be interesting to compare the two ligands and see how reactivity of these two ligands could be different. This is similar to the picket-fence porphyrin in theory, and might prove to be an effective strategy.[19-24, 41-42]

3.4 Experimental

3.4.1 General

All reactions and the following manipulations were carried out under anaerobic and anhydrous conditions with a nitrogen atmosphere by Schlenk or glovebox techniques (MBraun UNIlab Pro SP Eco equipped with a -40 ^{o}C freezer). Pentane, diethyl ether, dichloromethane, and tetrahydrofuran (Aldrich) were dried using an MBraun Solvent Purification System and stored over 4 Å molecular sieves for 24 hours prior to use. Acetonitrile (Aldrich) was distilled from calcium hydride and stored over 4 Å molecular sieves. Deuterated solvents (Cambridge Isotope Laboratories) were degassed and stored over 4 Å molecular sieves for 24 hours prior to use. Celite was dried by heating to >250 ^{o}C under dynamic vacuum for at least 24 hours prior to use.

NMR spectra were obtained using an Agilent Technologies 400 MHz spectrometer or a Varian Unity Inova 500 MHz spectrometer. Samples were referenced using the residual protio solvent peaks. UV-Vis spectroscopy was performed using a Shimadzu UV-2401PC spectrometer in a quartz cuvette containing a J. Young airtight adaptor.

Mass spectrometry was run at UCSB Chemistry's Mass Spectrometry Facility and all MALDI-TOF was run using a Microflex LRF MALDI TOF spectrometer with a 60 Hz nitrogen laser at 337nm. All ESI data was run on a Waters LCT Premier operated in positive mode by direct injection of the sample in either THF, acetonitrile, or methanol into the instrument.

3.4.2 Synthesis of Vanadyl 1,4,8,11,15,18, 22,25Octaethoxy-29H, 31H-phthalocyanine (V=OOEPC) (3.1)

A 100 mL Schlenk flask was charged with 500 mg (0.577 mmol) of **2.3**, 470 mg (2.883 mmol) of vanadyl sulfate, and 242.2 mg (2.883 mmol) of sodium bicarbonate. A solution was created by adding 50 mL of DMF. The solution was brought to reflux and refluxed for five hours. After five hours the solution was removed from heating and left to cool. Once cooled the solution was transferred to a 500 mL Erlenmeyer flask filled with 250 mL of DI water. This solution was allowed cool in the fridge overnight. After cooling, the product was filtered using a fine porosity frit. The solid product was washed with 30 mL of DI water, followed by 30 mL of ethanol, and 30 mL of ether. Yield: 0.380 g (0.408 mmol, 69%) ^{1}H NMR($CDCl_3$): δ 8.50 (bs, 8H, C_6H_2), 5.03 (bs, 16H, OCH_2), 1.88 ppm (bs, 8H, CH_3). ^{51}V NMR ($CDCl_3$): Silent. ESI (THF): $[M]^+$ 931.4 m/z, $[M+1]^+$ 932.4 m/z. LT-EPR (100K, DMF): $g_{||}$: 2.10, $g_{\perp}$: 2.00.

3.4.3 Synthesis of Vanadyl 1,4,8,11,15,18, 22,25Octaisopropoxy-29H, 31H-phthalocyanine (V=OOIPC)

A 100 mL schlenk flask was charged with 200 mg of **2.9** (0.204 mmol), 166 mg (1.018 mmol) of vanadyl sulfate, and 172 mg (2.047 mmol) of sodium bicarbonate. A solution was created by adding 20 mL of DMF. The solution was brought to reflux, and allowed to reflux. The solution was then pulled from heat and left to cool. 50 mL of DI water was added to the solution and it was moved to the fridge to cool overnight. The product was filtered off using a fine porosity frit. The product was then washed with 50 mL of DI water. Yield: 0.055 g (0.054 mmol, 26%) MALDI: $[M]^+$ 1043.4 m/z, $[M+1]^+$ 1044.4 m/z

3.5 Summary

This chapter described the synthesis and some characterization of two vanadyl alkoxy-substituted phthalocyanine species. Both of the vanadyl species were generated using similar methods using a vanadyl salt to replace the protons in the empty pocket of the phthalocyanine ligands. Attempts to synthesize a chromium-oxo species proved to be ineffective using both iodosobenzene and hypochlorite to attempt to oxidize the chromium phthalocyanine. Attempts from the manganese(III) chloride phthalocyanine were similarly ineffective in the synthesis of a manganese-oxo phthalocyanine. Despite the failure to isolate a manganese-oxo from the manganese(III) chloride phthalocyanine, the “naked manganese” species was much more reactive. Reactions with meta-chloroperbenzoic acid and oxygen show changes in the UV-Vis spectrum over time that could be the conversion to a manganese-oxo though isolation and full characterization of the produced species has been difficult.

3.6 References

1. Betley, T. A.; Wu, Q.; Van Voorhis, T.; Nocera, D. G., Electronic design criteria for O-O bond formation via metal-oxo complexes. *Inorg. Chem.* **2008,** *47* (6), 1849-1861.

2. O'Halloran, K. P.; Zhao, C. C.; Ando, N. S.; Schultz, A. J.; Koetzle, T. F.; Piccoli, P. M. B.; Hedman, B.; Hodgson, K. O.; Bobyr, E.; Kirk, M. L.; Knottenbelt, S.; Depperman, E. C.; Stein, B.; Anderson, T. M.; Cao, R.; Geletii, Y. V.; Hardcastle, K. I.; Musaev, D. G.; Neiwert, W. A.; Fang, X. K.; Morokuma, K.; Wu, S. X.; Kogerler, P.; Hill, C. L., Revisiting the Polyoxometalate-Based Late-Transition-Metal-Oxo Complexes: The "Oxo Wall" Stands. *Inorg. Chem.* **2012,** *51* (13), 7025-7031.

3. Liao, M. S.; Scheiner, S., Electronic structure and bonding in metal phthalocyanines, Metal=Fe, Co, Ni, Cu, Zn, Mg. *J. Chem. Phys.* **2001,** *114* (22), 9780-9791.

4. Liao, M. S.; Scheiner, S., Electronic structure and bonding in metal porphyrins, metal=Fe, Co, Ni, Cu, Zn. *J. Chem. Phys.* **2002,** *117* (1), 205-219.

5. Ramdhanie, B.; Stern, C. L.; Goldberg, D. P., Synthesis of the first corrolazine: A new member of the porphyrinoid family. *J. Am. Chem. Soc.* **2001,** *123* (38), 9447-9448.

6. Ramdhanie, B.; Zakharov, L. N.; Rheingold, A. L.; Goldberg, D. P., Synthesis, structures, and properties of a series of four-, five-, and six-coordinate cobalt(III) triazacorrole complexes: The first examples of transition metal corrolazines. *Inorg. Chem.* **2002,** *41* (16), 4105-4107.

7. Mandimutsira, B. S.; Ramdhanie, B.; Todd, R. C.; Wang, H. L.; Zareba, A. A.; Czemuszewicz, R. S.; Goldberg, D. P., A stable manganese(V)-oxo corrolazine complex. *J. Am. Chem. Soc.* **2002,** *124* (51), 15170-15171.

8. Goldberg, D. P.; Ramdhanie, B.; Mandimutsira, B. S.; Wang, H. L.; Fox, J. P., Corrolazines: Novel porphyrinoid compounds capable of oxygen binding, stabilization of high-valent metal-oxo species, and more. *J. Inorg. Biochem.* **2003,** *96* (1), 21-21.

9. Fox, J. P.; Ramdhanie, B.; Zareba, A. A.; Czernuszewicz, R. S.; Goldberg, D. P., Copper(III) and vanadium(IV)-Oxo corrolazines. *Inorg. Chem.* **2004,** *43* (21), 6600-6608.

10. Kerber, W. D.; Goldberg, D. P., High-valent transition metal corrolazines. *J. Inorg. Biochem.* **2006,** *100* (4), 838-857.

11. Goldberg, D. P., Corrolazines: New frontiers in high-valent metalloporphyrinoid stability and reactivity. *Acc. Chem. Res.* **2007,** *40* (7), 626-634.

12. McGown, A. J.; Badiei, Y. M.; Leeladee, P.; Prokop, K. A.; DeBeer, S.; Goldberg, D. P., Synthesis and Reactivity of High-Valent Transition Metal Corroles and Corrolazines. *Handb. Porphyr. Sci.* **2011,** *14*, 525-599.

13. Cho, K.; Leeladee, P.; McGown, A. J.; DeBeer, S.; Goldberg, D. P., A High-Valent Iron-Oxo Corrolazine Activates C-H Bonds via Hydrogen-Atom Transfer. *J. Am. Chem. Soc.* **2012,** *134* (17), 7392-7399.

14. Leeladee, P.; Jameson, G. N. L.; Siegler, M. A.; Kumar, D.; de Visser, S. P.; Goldberg, D. P., Generation of a High-Valent Iron Imido Corrolazine Complex and NR Group Transfer Reactivity. *Inorg. Chem.* **2013,** *52* (8), 4668-4682.

15. Joslin, E. E.; Zaragoza, J. P. T.; Siegler, M. A.; Goldberg, D. P., meso-N-Methylation of a porphyrinoid complex: activating the H-atom transfer capability of an inert Re-V(O) corrolazine. *Chem. Commun.* **2017,** *53* (12), 1961-1964.

16. Zaragoza, J. P. T.; Siegler, M. A.; Goldberg, D. P., A Reactive Manganese(IV)-Hydroxide Complex: A Missing Intermediate in Hydrogen Atom Transfer by High-

Valent Metal-Oxo Porphyrinoid Compounds. *J. Am. Chem. Soc.* **2018,** *140* (12), 4380-4390.

17. Lansky, D. E.; Mandimutsira, B.; Ramdhanie, B.; Clausen, M.; Penner-Hahn, J.; Zvyagin, S. A.; Telser, J.; Krzystek, J.; Zhan, R. Q.; Ou, Z. P.; Kadish, K. M.; Zakharov, L.; Rheingold, A. L.; Goldberg, D. P., Synthesis, characterization, and physicochernical properties of manganese(III) and manganese(V)-oxo corrolazines. *Inorg. Chem.* **2005,** *44* (13), 4485-4498.

18. Prokop, K. A.; Goldberg, D. P., Generation of an Isolable, Monomeric Manganese(V)-Oxo Complex from O-2 and Visible Light. *J. Am. Chem. Soc.* **2012,** *134* (19), 8014-8017.

19. Collman, J. P.; Gagne, R. R.; Halbert, T. R.; Marchon, J. C.; Reed, C. A., Reversible Oxygen Adduct Formation in Ferrous Complexes Derived from a Picket Fence Porphyrin - Model for Oxymyoglobin. *J. Am. Chem. Soc.* **1973,** *95* (23), 7868-7870.

20. Collman, J. P.; Gagne, R. R.; Gray, H. B.; Hare, J. W., Low-Temperature Infrared Spectral Study of Iron(Ii) Dioxygen Complexes Derived from a Picket-Fence Porphyrin. *J. Am. Chem. Soc.* **1974,** *96* (20), 6522-6524.

21. Collman, J. P.; Gagne, R. R.; Reed, C. A., Paramagnetic Dioxygen Complex of Iron(Ii) Derived from a Picket Fence Porphyrin - Further Models for Hemoproteins. *J. Am. Chem. Soc.* **1974,** *96* (8), 2629-2631.

22. Robinson, W. T.; Rodley, G. A.; Jameson, G. B., Structural Studies of Dioxygen Adducts of Picket Fence Porphyrins. *Acta Crystallogr., Sect. A: Found. Crystallogr.* **1975,** *31*, S49-S49.

23. Collman, J. P.; Gagne, R. R.; Reed, C. A.; Halbert, T. R.; Lang, G.; Robinson, W. T., Picket-Fence Porphyrins - Synthetic Models for Oxygen Binding Hemoproteins. *J. Am. Chem. Soc.* **1975,** *97* (6), 1427-1439.

24. Jameson, G. B.; Robinson, W. T.; Collman, J. P.; Sorrell, T. N., Crystal and Molecular-Structure of a Novel, High-Spin, Iron(Ii) Picket Fence Porphyrin Derivative - Catena-(Mu-[Meso-Tetrakis(Alpha-Alpha-Alpha-Alpha-Ortho-Pivalamidophenyl)-Porphinato-N,N',N',N'-O]-Aquoiron(Ii)-Tetrahydrothiophene). *Inorg. Chem.* **1978,** *17* (4), 858-864.

25. Dogutan, D. K.; McGuire, R.; Nocera, D. G., Electocatalytic Water Oxidation by Cobalt(III) Hangman beta-Octafluoro Corroles. *J. Am. Chem. Soc.* **2011,** *133* (24), 9178-9180.

26. Schwalbe, M.; Dogutan, D. K.; Stoian, S. A.; Teets, T. S.; Nocera, D. G., Xanthene-Modified and Hangman Iron Corroles. *Inorg. Chem.* **2011,** *50* (4), 1368-1377.

27. Dogutan, D. K.; Stoian, S. A.; McGuire, R.; Schwalbe, M.; Teets, T. S.; Nocera, D. G., Hangman Corroles: Efficient Synthesis and Oxygen Reaction Chemistry. *J. Am. Chem. Soc.* **2011,** *133* (1), 131-140.

28. Lai, W. Z.; Cao, R.; Dong, G.; Shaik, S.; Yao, J. N.; Chen, H., Why Is Cobalt the Best Transition Metal in Transition-Metal Hangman Corroles for O-O Bond Formation during Water Oxidation? *J. Phys. Chem. Lett.* **2012,** *3* (17), 2315-2319.

29. Contakes, S. M.; Beatty, S. T.; Dailey, K. K.; Rauchfuss, T. B.; Fenske, D., pi-complexes of phthalocyanines and metallophthalocyanines. *Organometallics* **2000,** *19* (23), 4767-4774.

30. Ghosh, S. K.; Patra, R.; Rath, S. P., Axial Ligand Coordination in Sterically Strained Vanadyl Porphyrins: Synthesis, Structure, and Properties. *Inorg. Chem.* **2008,** *47* (21), 9848-9856.

31. Ziolo, R. F.; Griffiths, C. H.; Troup, J. M., Crystal-Structure of Vanadyl Phthalocyanine, Phase-Ii. *J. Chem. Soc. Dalton Trans.* **1980,** (11), 2300-2302.

32. Golubkov, G.; Gross, Z., Chromium(V) and chromium(VI) nitrido complexes of tris(pentafluorophenyl)corrole. *Angew. Chem. Int. Ed.* **2003,** *42* (37), 4507-4510.

33. Liston, D. J.; Kennedy, B. J.; Murray, K. S.; West, B. O., Oxochromium Compounds .1. Synthesis and Properties of Mu-Oxo Chromium-Iron Porphyrin and Phthalocyanine Compounds. *Inorg. Chem.* **1985,** *24* (10), 1561-1567.

34. Groves, J. T.; Stern, M. K., Olefin Epoxidation by Manganese(Iv) Porphyrins - Evidence for 2 Reaction Pathways. *J. Am. Chem. Soc.* **1987,** *109* (12), 3812-3814.

35. Bortolini, O.; Meunier, B., Isolation of a High-Valent Oxo-Like Manganese Porphyrin Complex Obtained from Naocl Oxidation. *J. Chem. Soc. Chem. Comm.* **1983,** (22), 1364-1366.

36. Bortolini, O.; Ricci, M.; Meunier, B.; Friant, P.; Ascone, I.; Goulon, J., Isolation, Characterization and Structural Investigation by Exafs Xanes of High Valent Manganese Porphyrin Complexes as Active Species in the Naocl/Mn (Porphyrin) X-Oxygenation System. *Nouveau Journal De Chimie-New Journal of Chemistry* **1986,** *10* (1), 39-49.

37. Cortes, S. A.; Hernandez, M. A. M.; Nakai, H.; Castro-Rodriguez, I.; Meyer, K.; Fout, A. R.; Miller, D. L.; Huffman, J. C.; Mindiola, D. J., Titanium complexes supported by a sterically encumbering N-anchored tris-arylphenoxide ligand. *Inorg. Chem. Commun.* **2005,** *8* (10), 903-907.

38. Lambert, J. B.; Zhang, S. Z.; Ciro, S. M., Silyl Cations in the Solid and in Solution. *Organometallics* **1994,** *13* (6), 2430-2443.

39. Fujiki, M.; Tabei, H.; Isa, K., New Tetrapyrrolic Macrocycle - Alpha,Beta,Gamma-Triazatetrabenzcorrole. *J. Am. Chem. Soc.* **1986,** *108* (7), 1532-1536.

40. Li, J. Z.; Subramanian, L. R.; Hanack, M., Substituted alpha,beta,gamma-triazatetrabenzcorrole: An unusual reduction product of a phthalocyanine. *Chem. Commun.* **1997,** (7), 679-680.

41. Burke, J. M.; Kincaid, J. R.; Peters, S.; Gagne, R. R.; Collman, J. P.; Spiro, T. G., Structure-Sensitive Resonance Raman Bands of Tetraphenyl and Picket Fence Porphyrin-Iron Complexes, Including an Oxyhemoglobin Analog. *J. Am. Chem. Soc.* **1978,** *100* (19), 6083-6088.

42. Collman, J. P.; Brauman, J. I.; Doxsee, K. M.; Halbert, T. R.; Bunnenberg, E.; Linder, R. E.; Lamar, G. N.; Delgaudio, J.; Lang, G.; Spartalian, K., Synthesis and Characterization of Tailed Picket Fence Porphyrins. *J. Am. Chem. Soc.* **1980,** *102* (12), 4182-4192.